# A New Experiment for the HERA Collider
# Expression of Interest

H. Abramowicz[1], I. Abt[2], L. Adamczyk[3], M. Arneodo[4], J. Bracinik[2], A. Bruell[5], A. Caldwell[2,16], S. Chekanov[6], J. Chwastowski[7], J. Ciborowski[8], R. Devenish[9], Y. Eisenberg[10], A. Eskreys[7], J. Figiel[7], L. K. Gladilin[11], G. Grindhammer[2], G. Gustafson[12], D. Hasell[5], G. Ingelman[13], L. Jönsson[12], H. Jung[12], U. Karshon[10], C. Kiesling[2], E. Kinney[14], D. Kisielewska[3], H. Kowalski[15], A. Levy[1], X. Liu[16], L. Lönnblad[12], S. Magill[6], R. Milner[5], J. Repond[6], S. Schlenstedt[17], W. Schmidke[16], U. Schneekloth[15], W. Shekelian[2], T. Sjöstrand[12], L. Stanco[18], R. Stroili[18], J. Whitmore[19], R. Yoshida[6], L. Zawiejski[7]

T. Haas[15]

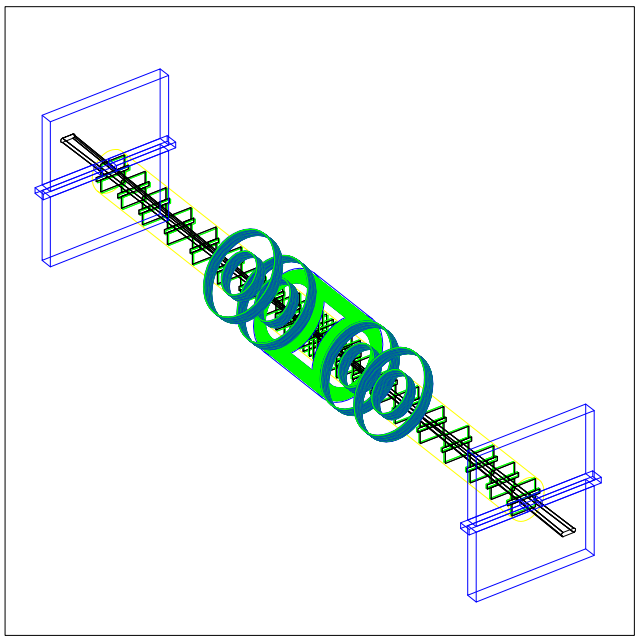

**A. Caldwell** **DESY PRC meeting** **May 7,2003**

1 Tel Aviv University, Tel Aviv, Israel
2 Max-Planck-Institut für Physik, Werner-Heisenberg-Institut, Munich, Germany
3 University of Mining and Metallurgy, Cracow, Poland
4 University of Eastern Piedmont, Novara and INFN Torino, Italy
5 Massachussetts Institute of Technology, Cambridge, USA
6 Argonne National Laboratory, Argonne, USA
7 Institute of Nuclear Physics, Cracow, Poland
8 Warsaw University, Warsaw, Poland
9 University of Oxford, Oxford, United Kingdom
10 Weizmann Institute, Rehovot, Israel
11 Moscow State University, Institute of Nuclear Physics, Moscow, Russia
12 Lund University, Lund, Sweden
13 Uppsala University, Uppsala, Sweden
14 University of Colorado, Boulder, USA
15 Deutsches Elektronen-Synchrotron DESY, Hamburg, Germany
16 Columbia University, New York, USA
17 DESY Zeuthen, Zeuthen, Germany
18 University of Padova, Padova, Italy
19 Pennsylvania State University, University Park, USA

# Physics Motivation– Strong Interactions

• QCD is the most complex of the forces operating in the microworld ⇒ expect many beautiful and strange effects

• QCD is fundamental to the understanding of our universe: source of mass (relation to gravity ?), confinement of color, …

• We need to understand radiation processes in QCD, both at small distance scales and large.

  • small distance scales: understand parton splitting (DGLAP, BFKL, CCFM, …)

  • larger distance scales: suppression of radiation, transition to non-perturbative regime (constituent quarks, …)

• Observation of the saturated gluon state (color glass condensate) ? Expected to be a universal state of matter.

# HERA Kinematics

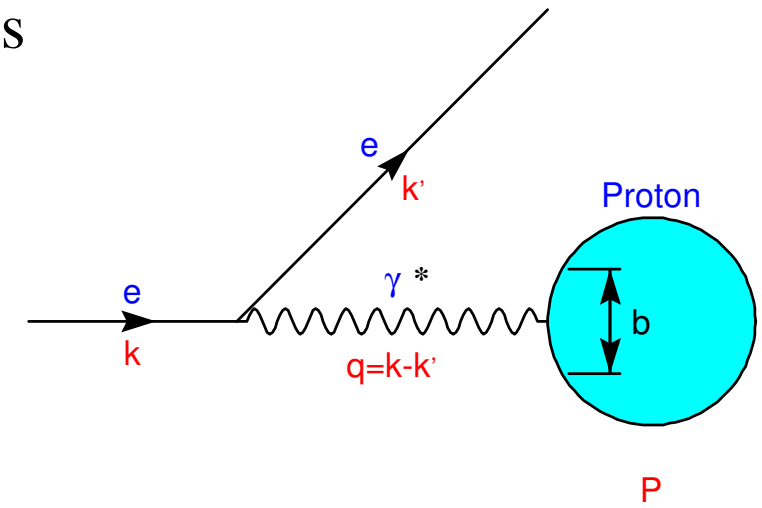


**$E_e$=27.5 GeV**
**$E_P$=920 GeV**

**$s=(k+P)^2 = (320\ GeV)^2$** — **CM energy squared**
**$Q^2=-(k-k`)^2$** — **virtualiy**
**$W^2=(q+P)^2$** — **$\gamma^*P$ CM energy squared**

**Transverse distance scale probed: $b \approx \hbar c/Q$**

| | | |
|---|---|---|
| **McAllister, Hofstadter** | **Ee=188 MeV** | **$b_{min}$=0.4 fm** |
| **Bloom et al.** | **10 GeV** | **0.05 fm** |
| **CERN, FNAL fixed target** | **500 GeV** | **0.007 fm** |
| **HERA** | **50 TeV** | **0.0007 fm** |

## Proton inf mom frame

## Proton rest frame

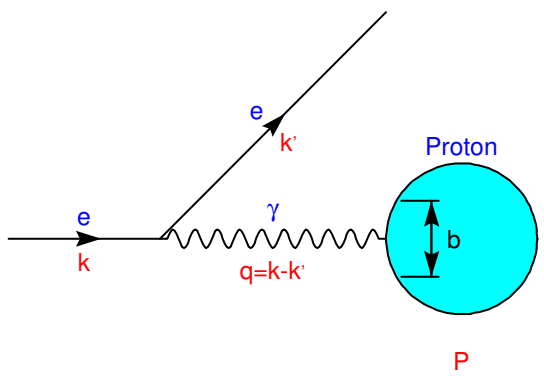


**$x=Q^2/2P\,q$** **fraction on P momentum carried by struck quark**

**$\tau = 1/2M_p x = W^2/2M_P Q^2$** **Lifetime of hadronic fluctuations of photon**

**Radiation cloud surrounds both photon, proton ⇒ universal property of nature**

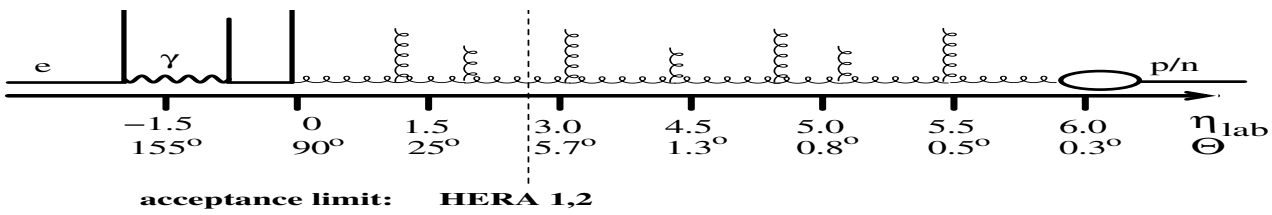

## Proton inf mom frame

Rutherford

$$d^2\sigma/dxdQ^2=2\pi\alpha^2/xQ^4[(1+(1-y)^2)F_2 - y^2F_L]$$

$F_2 = \Sigma_f e^2_f \, x \, \{q(x,Q^2) + \bar{q}(x,Q^2)\}$
$e_f$ is quark charge
$q(x,Q^2)$ is quark density

$F_L = 0$ in LO (QPM), non-zero after gluon radiation. Key test of our understanding

## Proton rest frame

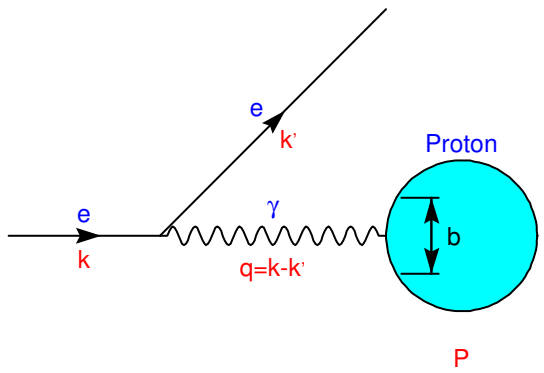


$d^2\sigma/dW\,dQ^2 = \Gamma\ (\sigma_T + \varepsilon\,\sigma_L)$

$\Gamma$ is flux of photons

$\sigma_{T,L}$ are cross sections for transversely, longitudinally polarized photons to scatter from proton

$\varepsilon$ is the relative flux

$$F_2 = Q^2/4\pi^2\alpha\ (\sigma_T + \varepsilon\,\sigma_L)$$

# Physics Picture in Proton Rest Frame

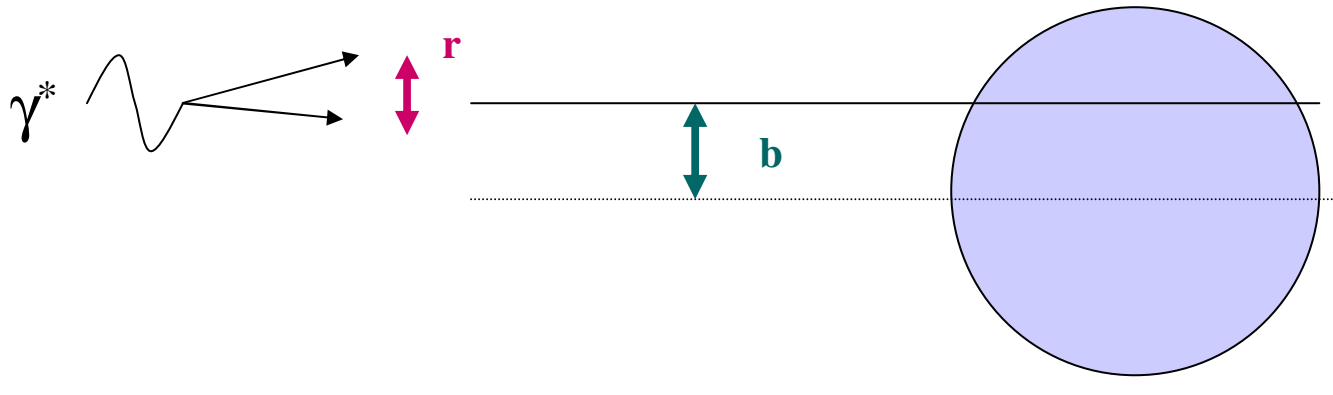


**r ~ 0.2 fm/Q (0.02 – 2 fm for 100>Q $^2$>0.01 GeV $^2$) transverse size of probe**

**ct ~ 0.2 fm (W $^2$/2M$_P$Q$^2$ ) (<1 fm to 1000‘s fm) – scale over which photon fluctuations survive**

**And, in exclusive processes, can vary the impact parameter**

**b ~ 0.2 fm/ sqrt(t ) t=(p -p‘)$^2$**

**Can control these parameters experimentally ! Can scan the distribution of strongly interacting matter in hadrons.**

# Hadron-hadron scattering cross section versus CM energy

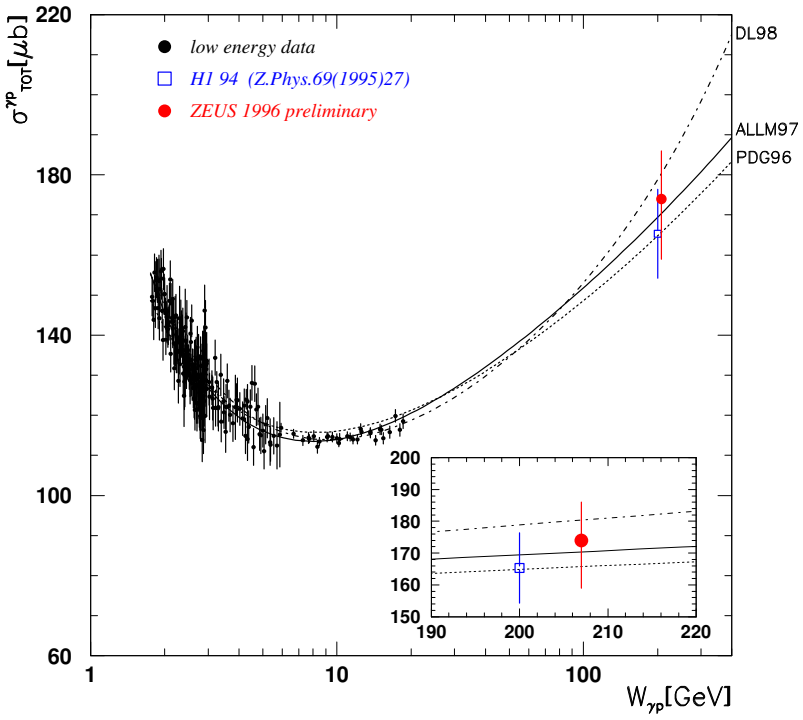


**$\gamma^*$P scattering cross section versus CM energy ($Q^2 \approx 0$). Same energy dependence observed**

$s^{0.08}$ vs $W^{2\ 0.08}$

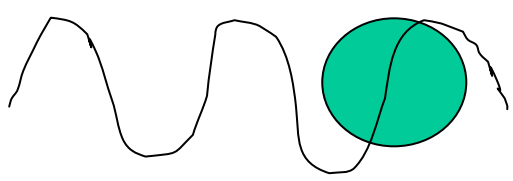

**Don't see partons**

# Cross sections as a function of $Q^2$

The rise of $F_2$ with decreasing x observed at HERA is strongly dependent on $Q^2$

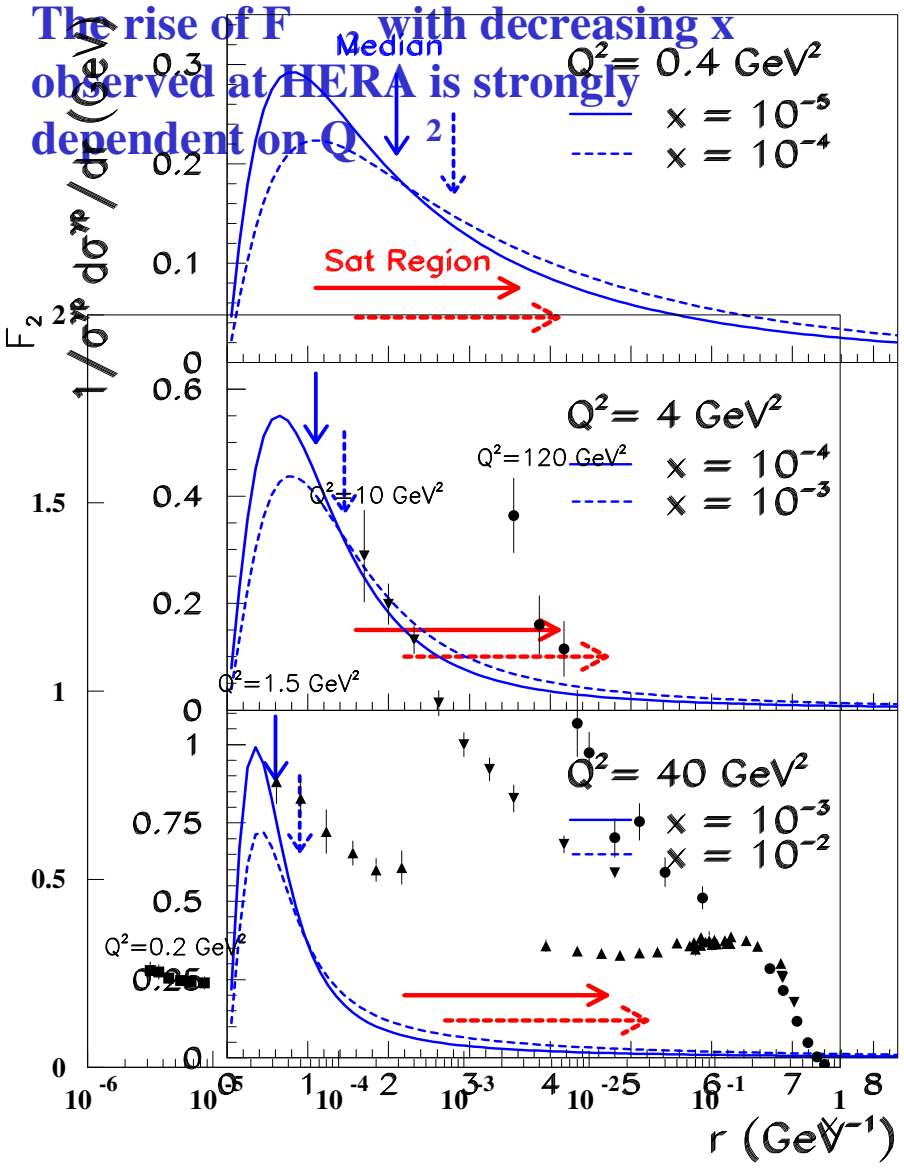


FIG. 8: The distribution of the dipole sizes contributing to the inclusive total cross-section at various virtualities $Q^2$ and some representative $x$ values. The vertical arrows indicate the median radius of a dipole which scatters off the proton. The horizontal arrows indicate saturation region $r > r_s(b,x)$ at $b = 0$. See Table II.

which has the simple interpretation as the amplitude for diffractive vector meson production from the elastic scattering of a dipole of radius $r$. The overlap function is shown in Fig. 7 for the transverse component of the three $J/\psi$ wave-functions considered in the paper.

### G. Dipole size

To interpret the IP Saturation model physically, we determined the typical dipole size contributing to the total cross-section. The distribution of dipole sizes $\frac{1}{\sigma^{\gamma^* p}}\frac{d\sigma^{\gamma^* p}}{dr}$ is the integrand of Eq. 5 after the $z$ integration is performed. Figure 8 shows this distribution at representative values of $x$ and $Q^2$. For each illustrated $x$ and $Q^2$ the arrow indicates the median radius of a dipole which

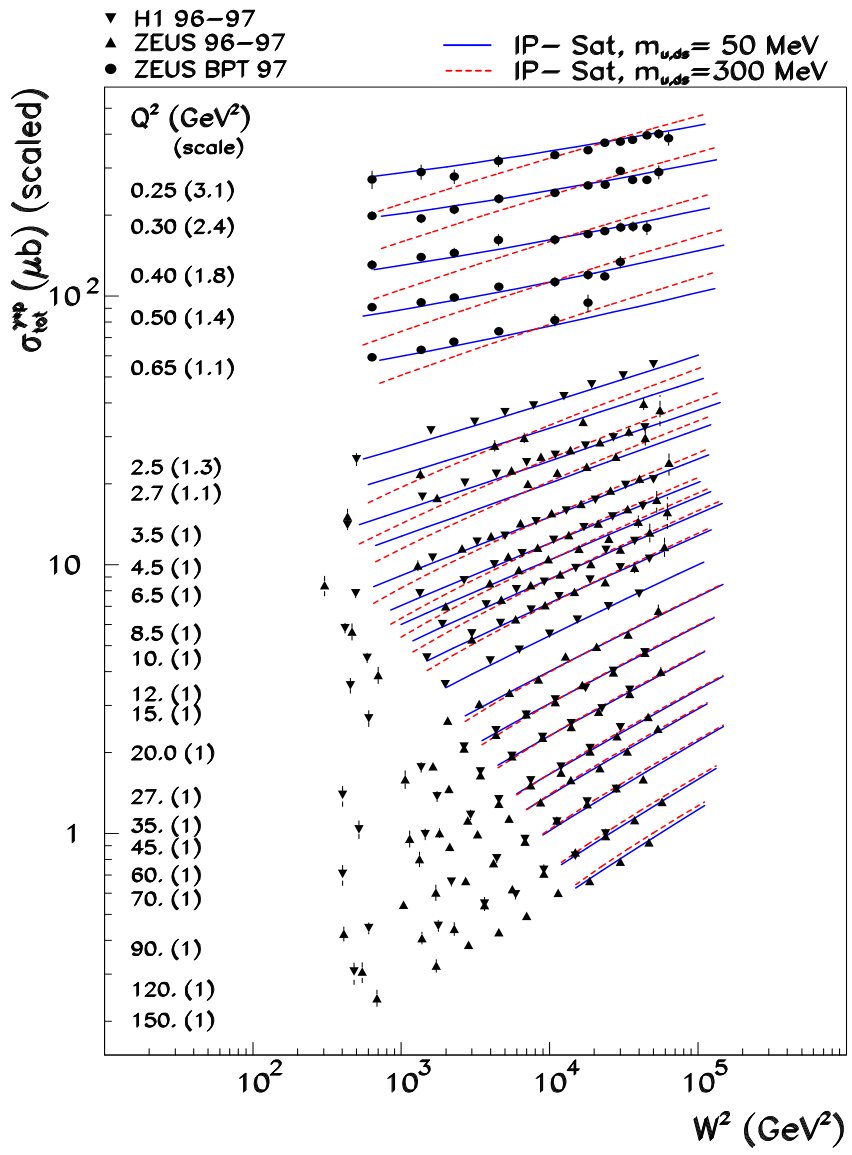


Equivalently, strongly rising $\gamma^* p$ cross section with W at high $Q^2$

FIG. 9: The total cross section as a function of $W^2$ at various $Q^2$. The values of $Q^2$ are shown on the left side of the plot along with the scale factor applied to the data for a better visibility. The full (dashed) line shows a fit by the IP Saturation Model with $m_{u,d,s} = 50$ MeV ($m_{u,d,s} = 300$ MeV). The fits are performed for $x < 0.01$.

scatters off the proton. Note that at smallest $Q^2$ and $x = 10^{-5}$ the majority of dipoles are smaller than $r \lesssim 2$ GeV$^{-1}$ and thus half of the dipoles are perturbative.

## IV. RESULTS FOR $\gamma^* p$ PROCESSES

### A. Inclusive total cross-section

The fit to the total $\gamma^* p$ cross-section data was performed in the range $x < 0.01$ and $Q^2 > 0.25$ GeV$^2$. The small $x$ cut leads to an upper limit on $Q^2$, $Q^2 < 200$ GeV$^2$. Figure 9 shows the $\gamma^* p$ cross section as a function of $W^2$ at the various $Q^2$ measured by the HERA experiments [29]. Following the rise of the total cross section with $W^2$ at fixed $Q^2$, we observe a striking change: for small $Q^2$ (the top of Fig. 9) the cross section rises slowly with the center of mass energy $W^2$, while for large $Q^2$ (the bottom of Fig. 9) the cross section rises strongly. If

# The behavior of the rise with $Q^2$

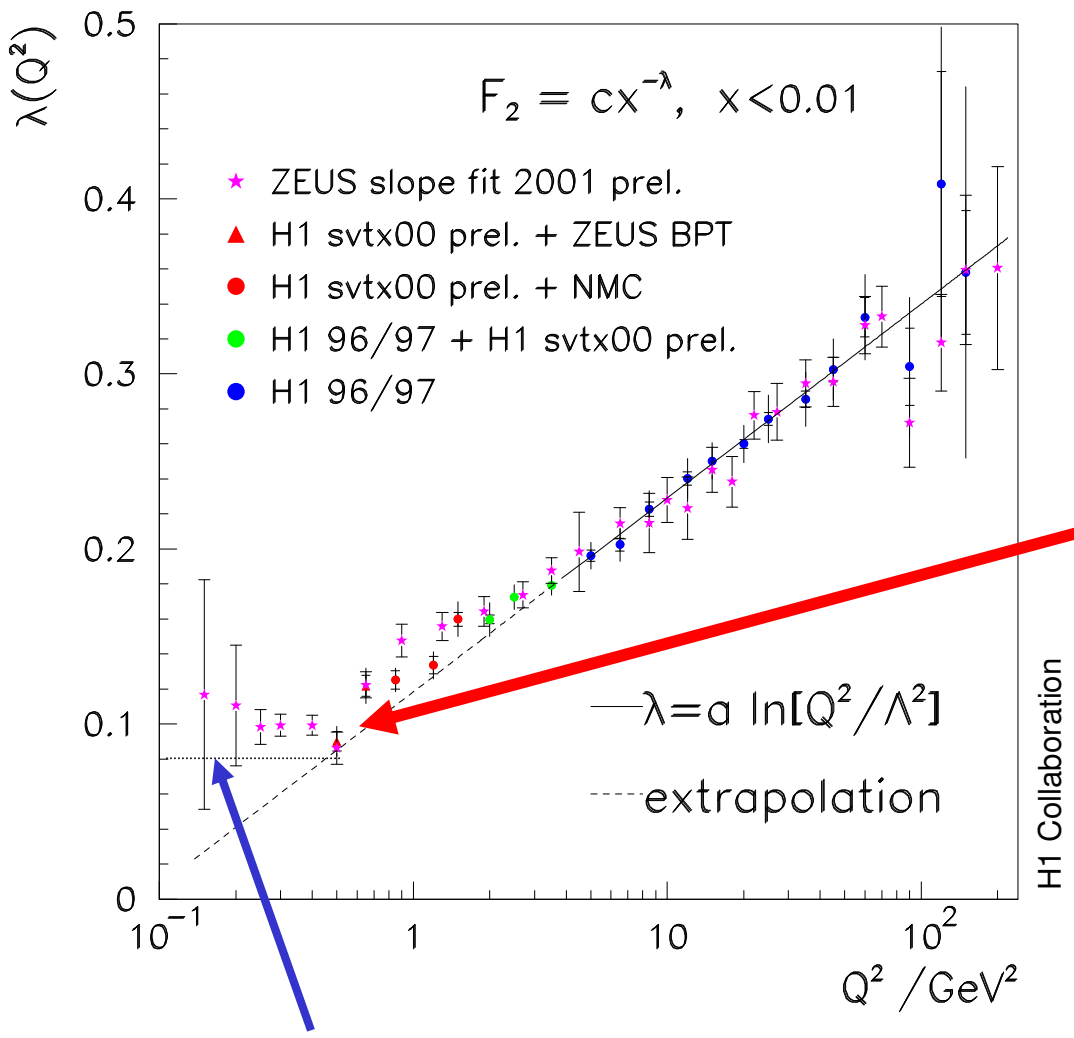


**Below $Q^2 \approx 0.5$ GeV$^2$, see same energy dependence as observed in hadron - hadron interactions. Observe transition from partons to hadrons (constituent quarks) in data. Distance scale ≈ 0.3 fm ??**

**What physics causes this transition ?**

**Hadron-hadron scattering energy dependence (Donnachie-Landshoff)**

# Analysis of $F_2$ in terms of parton densities (quarks and gluons)

**NLO DGLAP fits can follow the data accurately, yield parton densities.**
**BUT:**

- **many free parameters (18-30)**

- **form of parametrization fixed (not given by theory)**

**Constraints, e.g., $d_{sea}=u_{sea}$ put in by hand. Is this correct ? Need more constraints to untangle parton densities.**

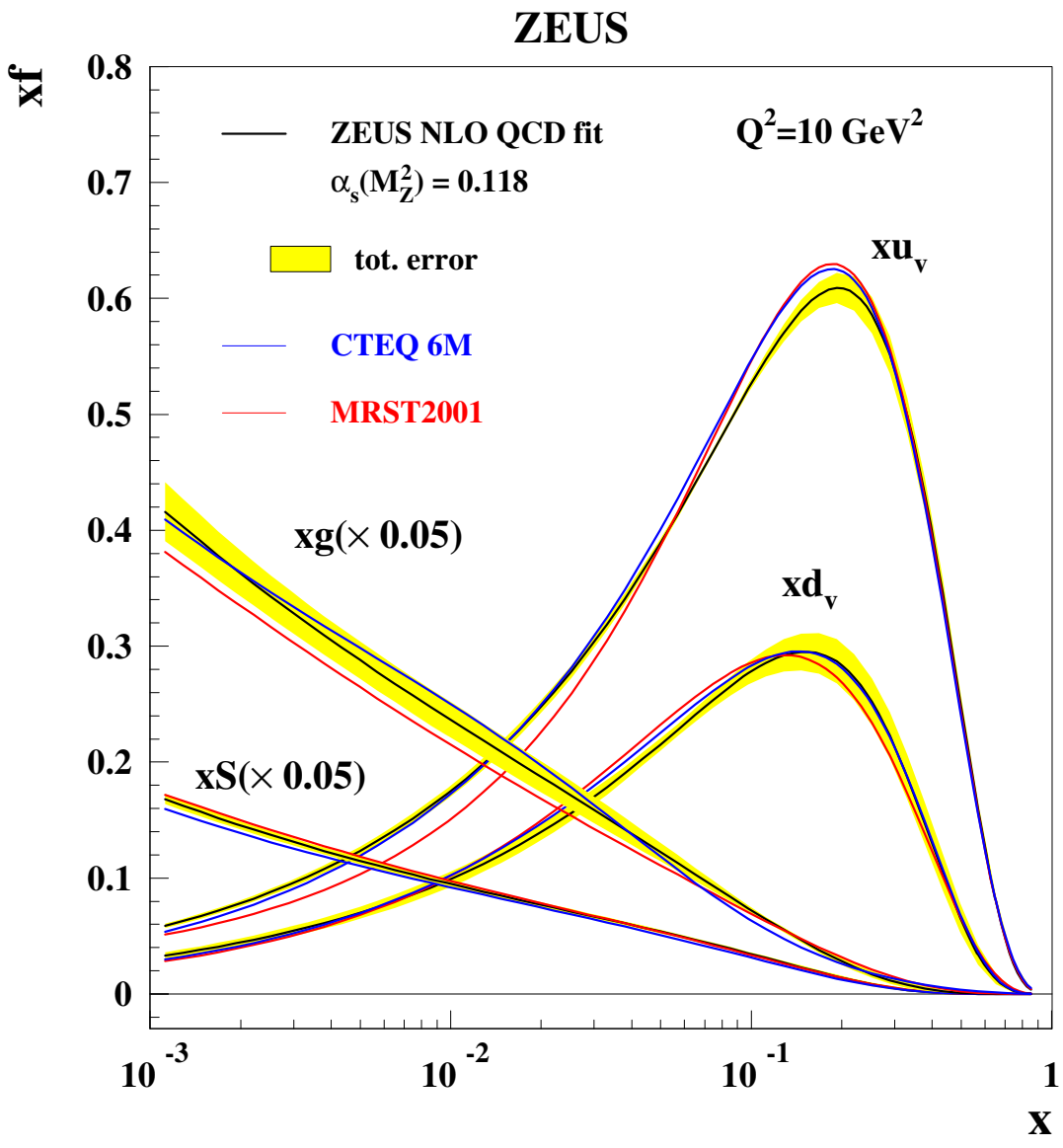

# See breakdown of pQCD approach ...

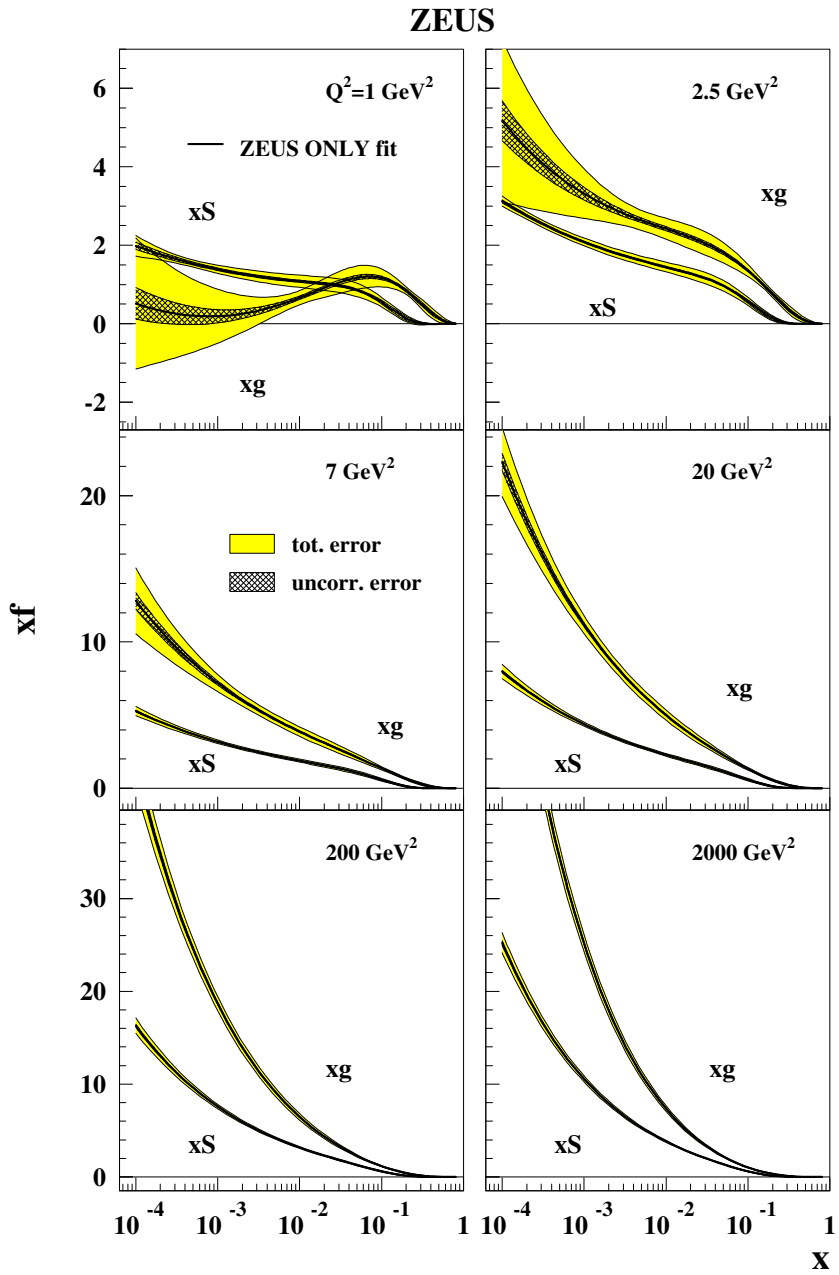


**Gluon density known with good precision at larger $Q^2$. For $Q^2$=1, gluons go negative. NLO, so not impossible, BUT – cross sections such as $\sigma_L$ also negative !**

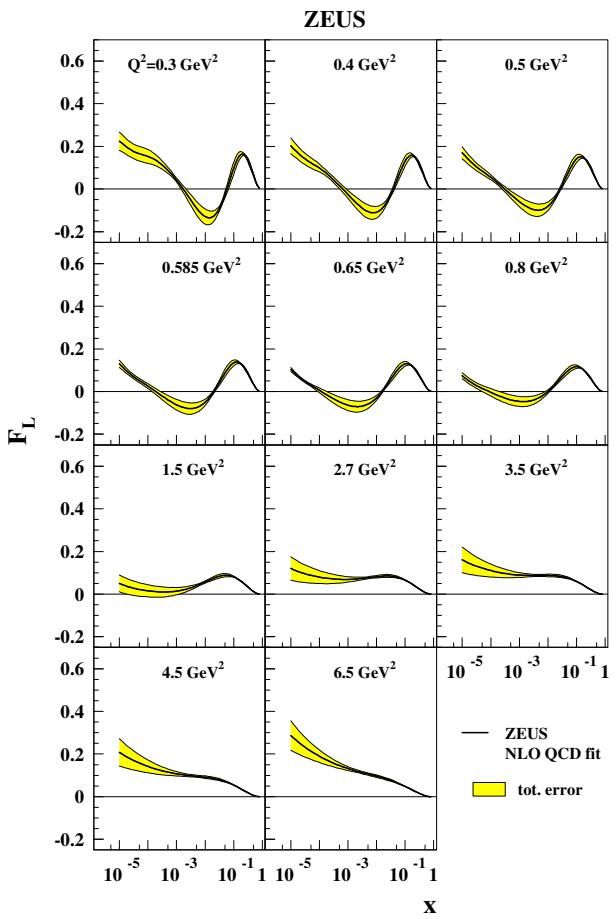

**We need to test N$^k$LO DGLAP fits and extraction of gluon densities. Crucial, since DGLAP is our standard tool for calculating PDF's in unmeasured regions.**

**Gluon densities not known at higher order, low $Q^2$. Need more precise measurements, additional observables (e.g., $F_L$)**

Thorne

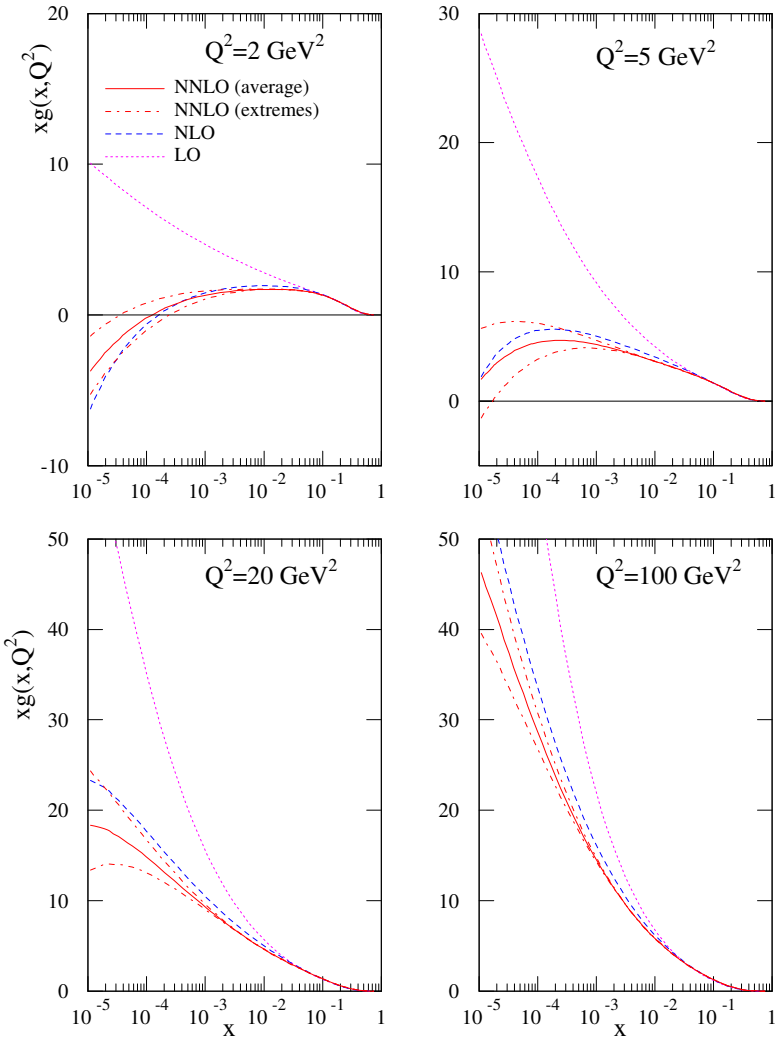

**$F_L$ shows tremendous variations when attempt to calculate at different orders. But $F_L$ is an observable – unique result.**

**Problem: $F_2$ NLO DGLAP fits work well, but large number of free parameters. Do we really know the gluon density ? Need to show that we can make accurate predictions for cross sections.**

**$F_L$ very sensitive observable – let's measure it**

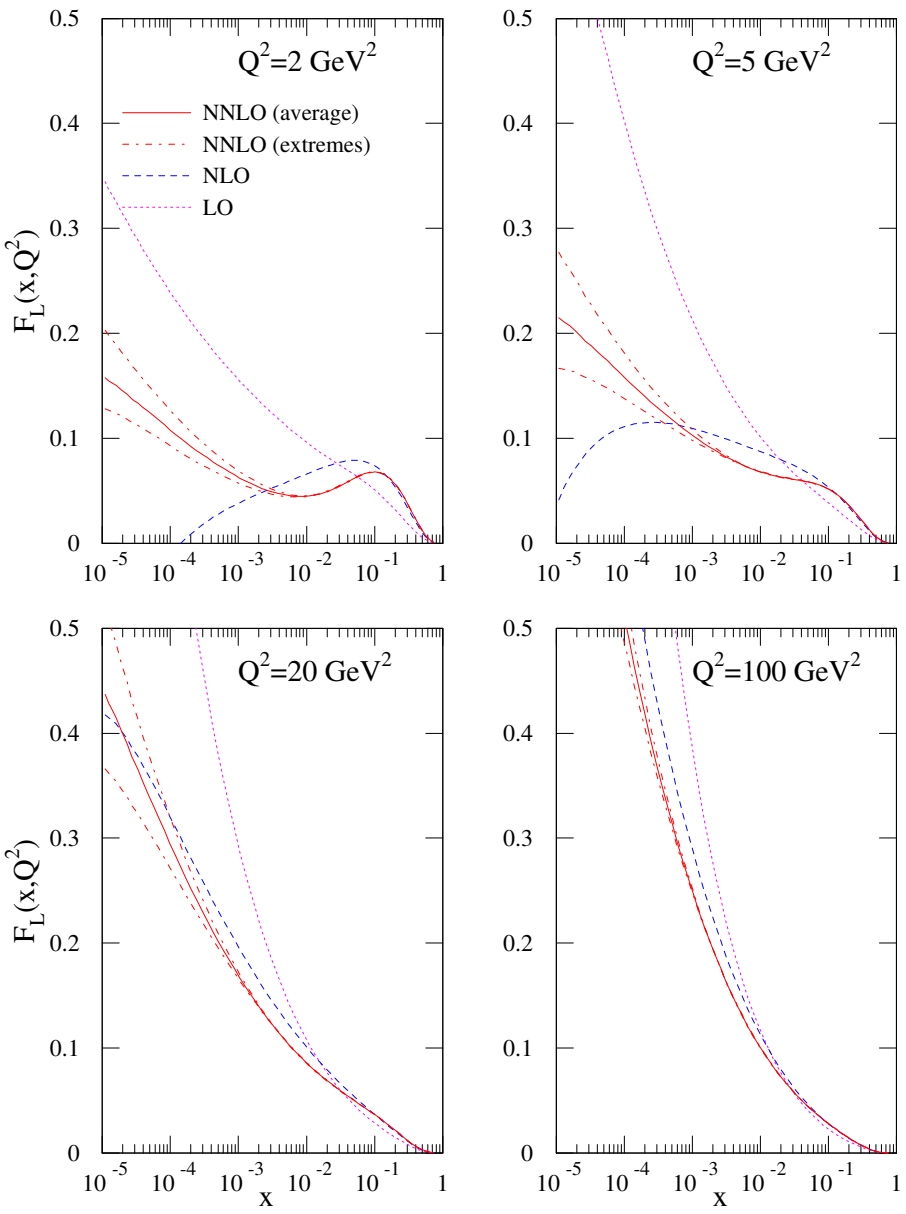

# Diffractive Surprises

‘Standard DIS event’

**Detector activity in proton direction**

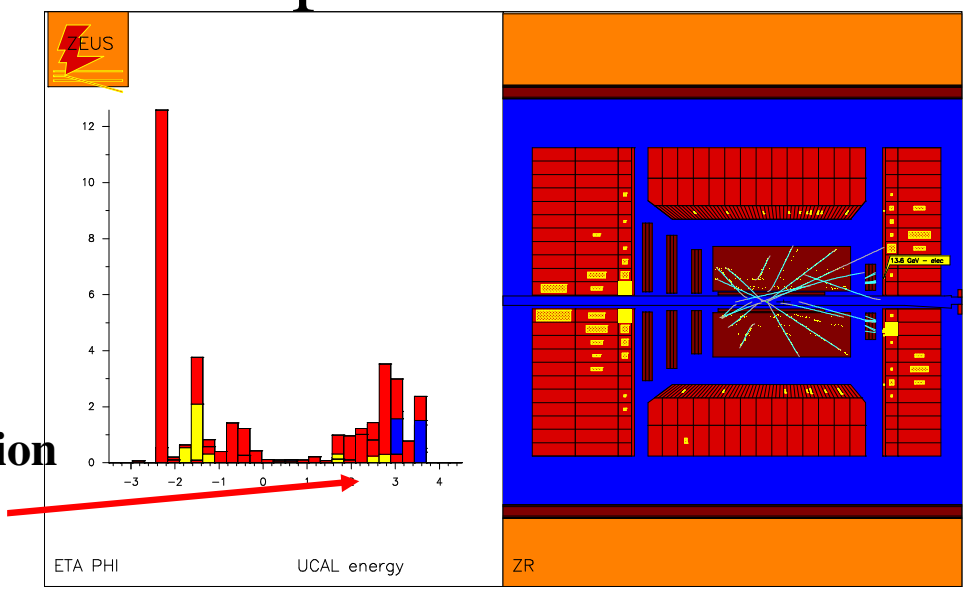


Diffractive event

**No activity in proton direction**

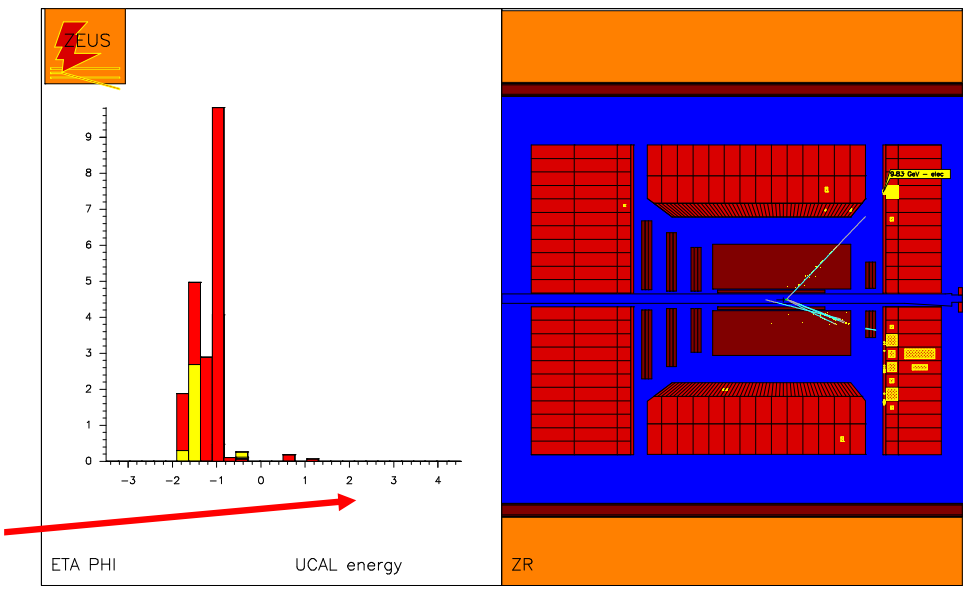

# Diffraction

1. **There is a large diffractive cross section, even in DIS (ca. 20 %)**
2. **The diffractive and total cross sections have similar energy dependences. Data suggests simple physics – what is it ?**

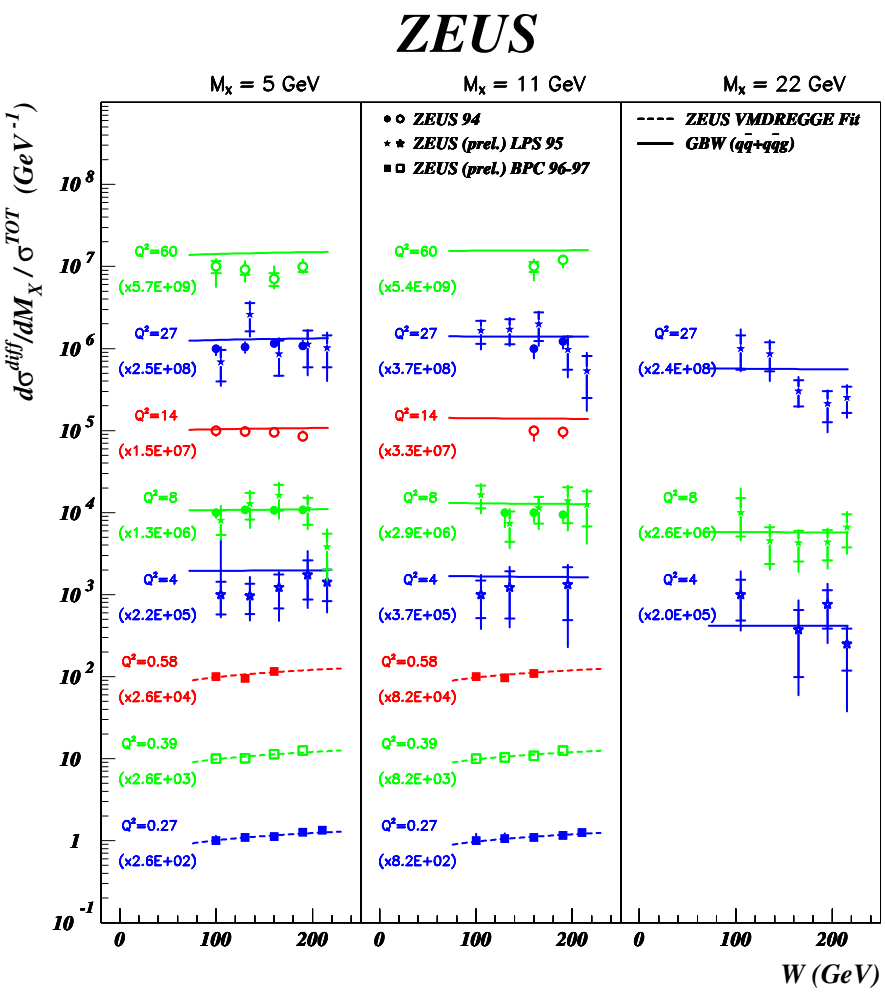


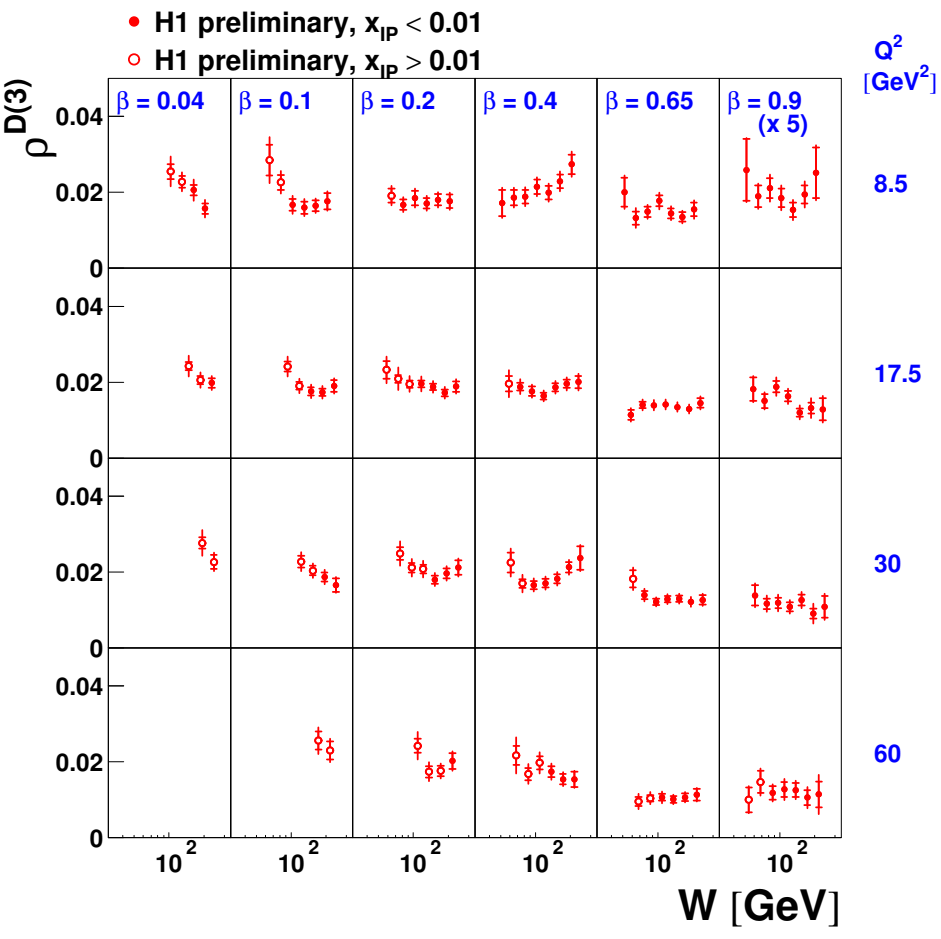

- Exclusive Processes (VM and DVCS)

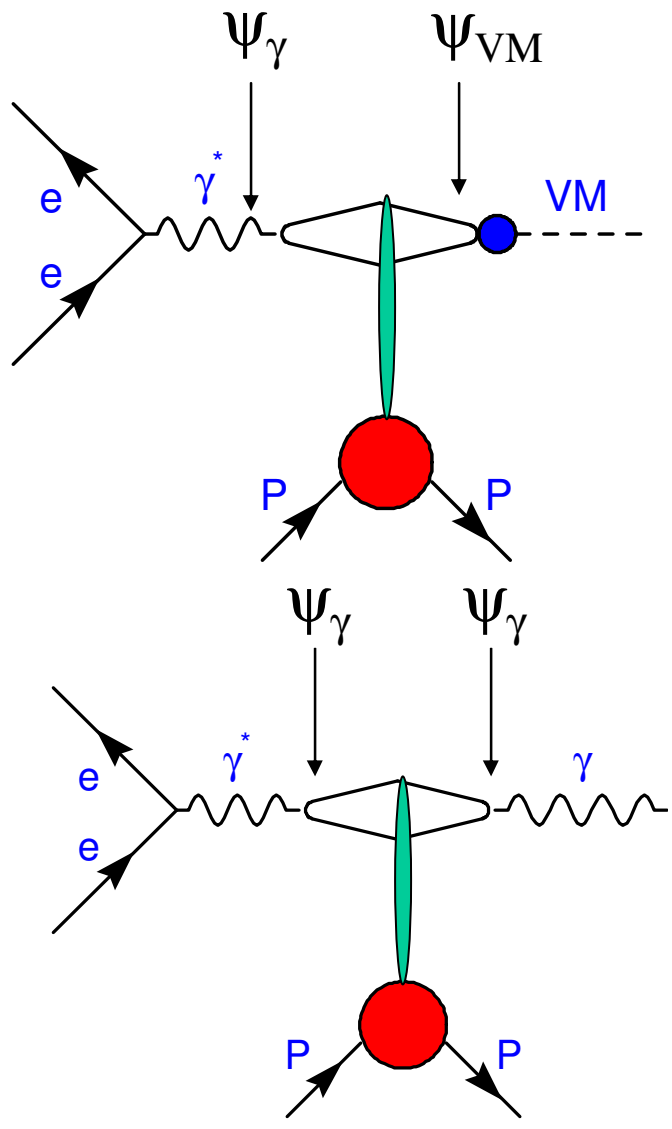


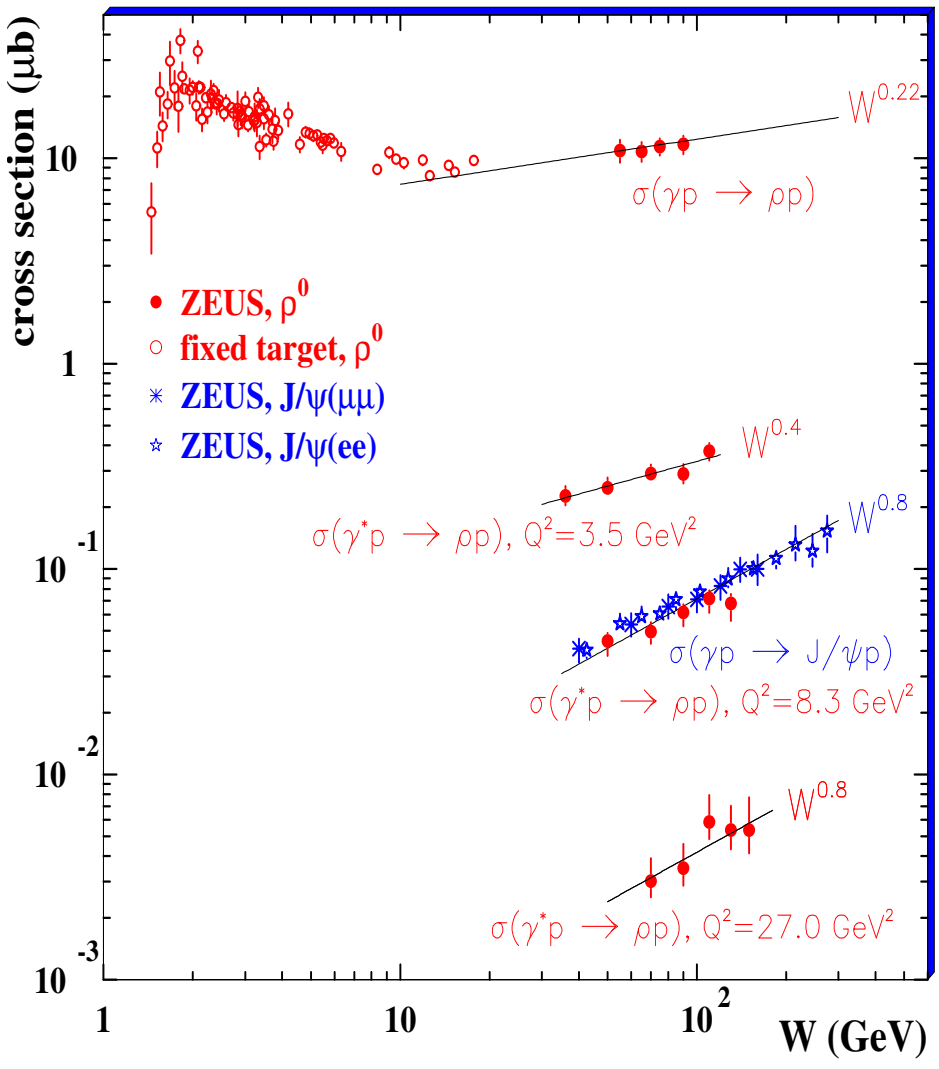

## Energy dependence of exclusive processes

**$ep \rightarrow eVp$ ($V = \rho, \omega, \phi, J/\psi$)  $ep \rightarrow e\gamma p$ (as QCD process)**

**ZEUS**

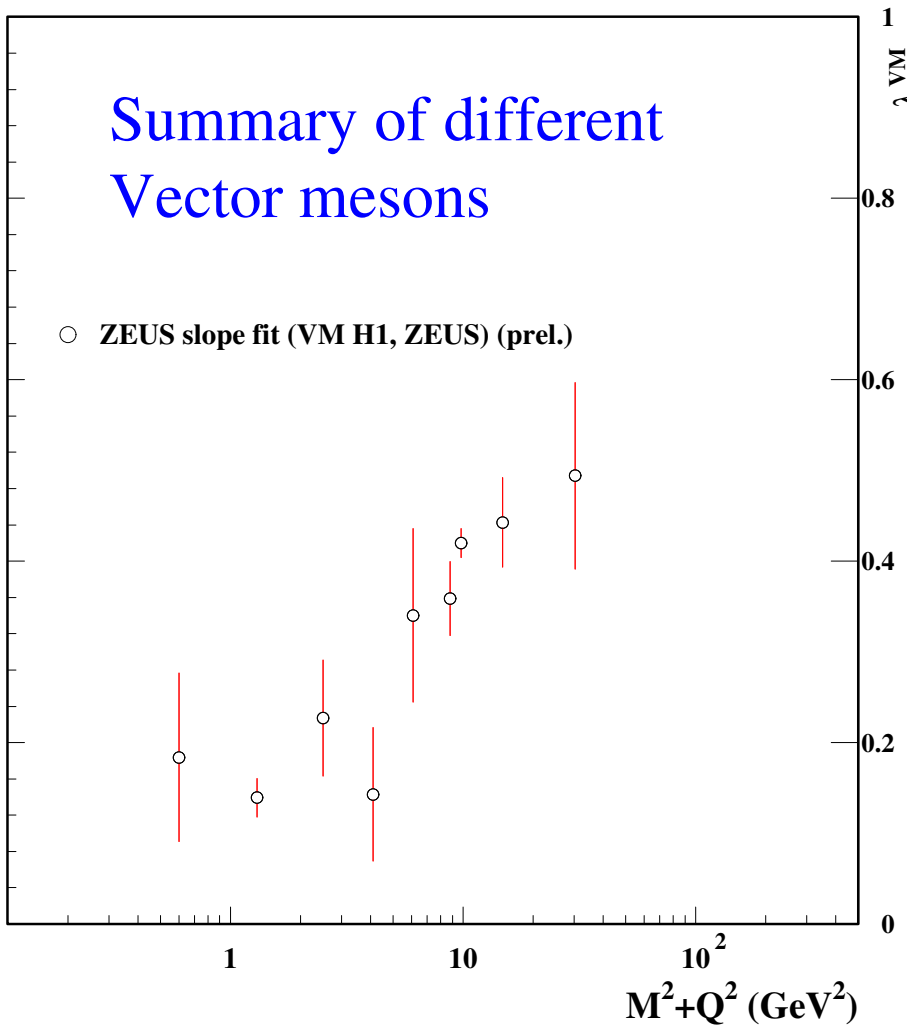


**Rise similar again to that seen in total cross section.**

**Need bigger lever arm in W to see energy dependence more precisely.**

**Need to distinguish elastic from proton dissociation events for small impact parameter scans of proton.**

Consider interaction of $q\bar{q}$ with proton (viewed in proton rest frame):

## Dipole Model for DIS:

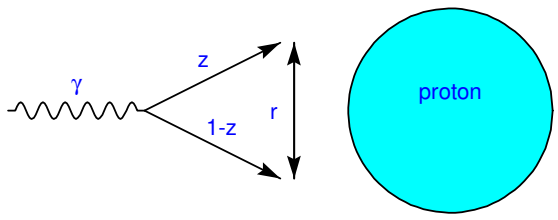


1. photon wavefunction, $\Psi(Q, z, r)$ can be calculated
2. parametrize $q\bar{q}$ scattering on proton

$$\hat{\sigma} = \sigma_0(1 - e^{-r^2/4R_0(x)^2})$$

**Golec-Biernat. Wuesthoff**

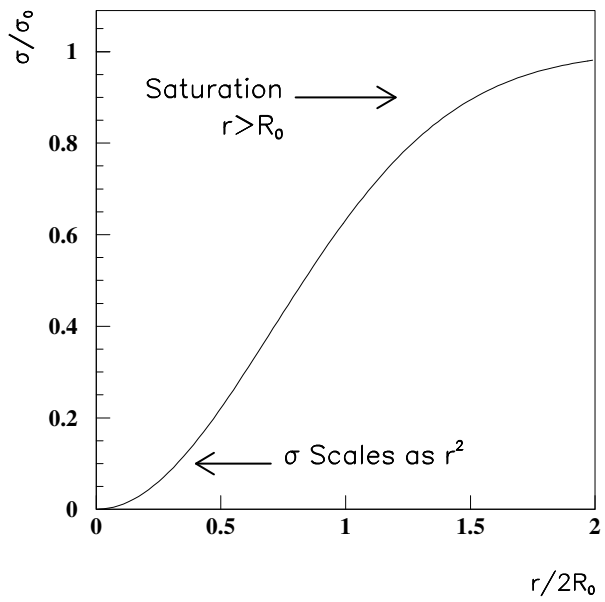

$R_0$ is parametrized as

$$R_0^2(x) = \left(\frac{x}{x_0}\right)^{\lambda}$$

For $\lambda > 0$, saturation at small-$x$. There are three free parameters in the model (+ quark masses), $\sigma_0, \lambda, x_0$ which are tuned on $F_2$ data.

The total $\gamma^* p$ cross section is calculated as:

$$\sigma_{L,T}(Q,W) = \int d^2\vec{r} \int dz |\Psi_{L,T}(Q,z,r)|^2 \sigma_{q\bar{q}-p}$$

for longitudinally (L) or transversely (T) polarized photon.

The diffractive cross section is calculated as:

$$\frac{d\sigma_{L,T}^{Diff}(Q,W)}{dt}|_{t=0} = \frac{1}{16\pi} \int d^2\vec{r} \int dz |\Psi_{L,T}(Q,z,r)|^2 \sigma_{q\bar{q}-p}^2$$

and Vector Meson production is calculated as:

$$\begin{aligned} A_{L,T} &= \int dz \int d^2\vec{r}\ \Psi_V^{*L,T}(r,z)\ \sigma_{q\bar{q}-p}\ \Psi_\gamma^{L,T}(Q,r,z) \\ \frac{d\sigma}{dt}|_{t=0} &= \frac{|A|^2}{16\pi} \end{aligned}$$

So that in principle we have sensitivity separately to the photon wave-function and the dipole-proton scattering cross section.

**More recent advances:**

- **add gluon evolution to cross section (DGLAP)**
- **add impact parameter dependence**

**Profile function:**

**Gaussian example:**

**Fix parameters of T(b) from exclusive J/ψ production**

**Gluon density parameters fixed with $F_2$ (or $\sigma_{\gamma P}$)**

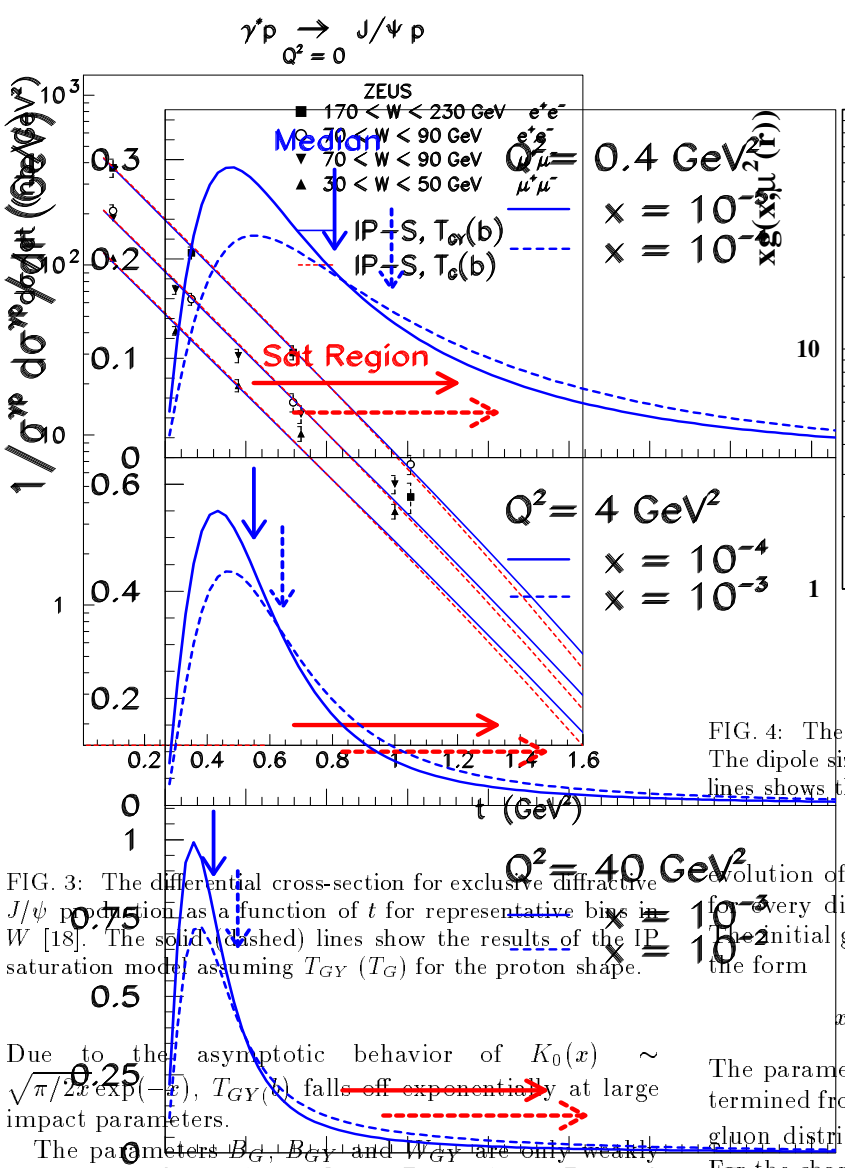


FIG. 3: The differential cross-section for exclusive diffractive $J/\psi$ production as a function of $t$ for representative bins in $W$ [18]. The solid (dashed) lines show the results of the IP saturation model assuming $T_{GY}$ ($T_G$) for the proton shape.

Due to the asymptotic behavior of $K_0(x) \sim \sqrt{\pi/2x}\exp(-x)$, $T_{GY}(b)$ falls off exponentially at large impact parameters.

The parameters $B_G$, $B_{GY}$ and $W_{GY}$ are only weakly dependent on the other parameters in the model and were determined iteratively. From the fit to the limited $t$ range, $|t| < 0.7$ GeV$^2$, the following values were found: $B_G = 4.25$ GeV$^{-2}$ for $T_G(b)$ and $B_{GY} = 3.25$ GeV$^{-2}$ and $W_{GY} = 0.66$ GeV$^{-1}$ for $T_{GY}(b)$. Figure 3 shows a representative subset of data [18] together with the results of a fit to the data using both forms of $T(b)$.

FIG. 8: The distribution of the dipole sizes contributing to the inclusive total cross-section at various virtualities $Q^2$ and some representative $x$ values. The vertical arrows indicate the median radius of a dipole which scatters off the proton. The horizontal arrows indicate saturation region $r > r_s(b, x)$ at $b = 0$. See Table II.

### C. Gluon Structure Function and Dipole Evolution

The dipole cross-section (Eq. 16) requires the gluon density $xg(x, \mu^2)$ for all scales $\mu^2$. As in previous work [2], the scale $\mu^2$ is related to the dipole size by

$$\mu^2 = \frac{C}{r^2} + \mu_0^2 \qquad (20)$$

which has the simple interpretation as the amplitude for diffractive vector meson production from the elastic scattering of a dipole of radius $r$. The overlap function is shown in Fig. 7 for the transverse component of the three $J/\psi$ wave-functions considered in the paper.

The gluon density is evolved to the scale $\mu^2$ with leading order DGLAP without quarks for the gluon density. The evolution of the gluon density is performed numerically for every dipole size $r$ during the integration of Eq. 5. The initial gluon distribution is taken at the scale $\mu_0^2$ in the form

$$xg(x, \mu_0^2) = A_g x^{-\lambda_g}(1-x)^{5.6}. \qquad (21)$$

The parameters of the model $C$, $\mu_0^2$, $A_g$, and $\lambda_g$ are determined from a fit to the DIS data. For light quarks the gluon distribution is evaluated at $x = x_{BJ} = \frac{Q^2}{Q^2+W^2}$. For the charm quark the gluon structure function is evaluated at $x = (4m_c^2 + Q^2)/(Q^2 + W^2)$, where $m_c$ is the charm quark mass [19]. This implies that the dipole cross section is flavor dependent when performing the sum over flavors in Eq. 5.

The present model has, in some sense, one less parameter than the model of Ref. [2]. The parameter $\sigma_0$ which previously determined the asymptotic size of the dipole cross-section is now replaced by the parameter $B_G$ (or $B_{GY}$ and $W_{GY}$) which is (are) fixed by the shape of the diffractive $t$-distribution.

The gluon structure function obtained from the fit is shown in Fig. 4 for various dipole sizes. The dipole size determines the evolution scale $\mu^2$ through Eq. 20. QCD evolution changes the rate of rise of the gluon structure function $xg(x, \mu^2)$. The rate of rise is usually quantified by the exponent $\lambda_{eff}$,

$$\lambda_{eff} = \frac{d\log xg(x,\mu^2)}{d\log(1/x)}. \qquad (22)$$

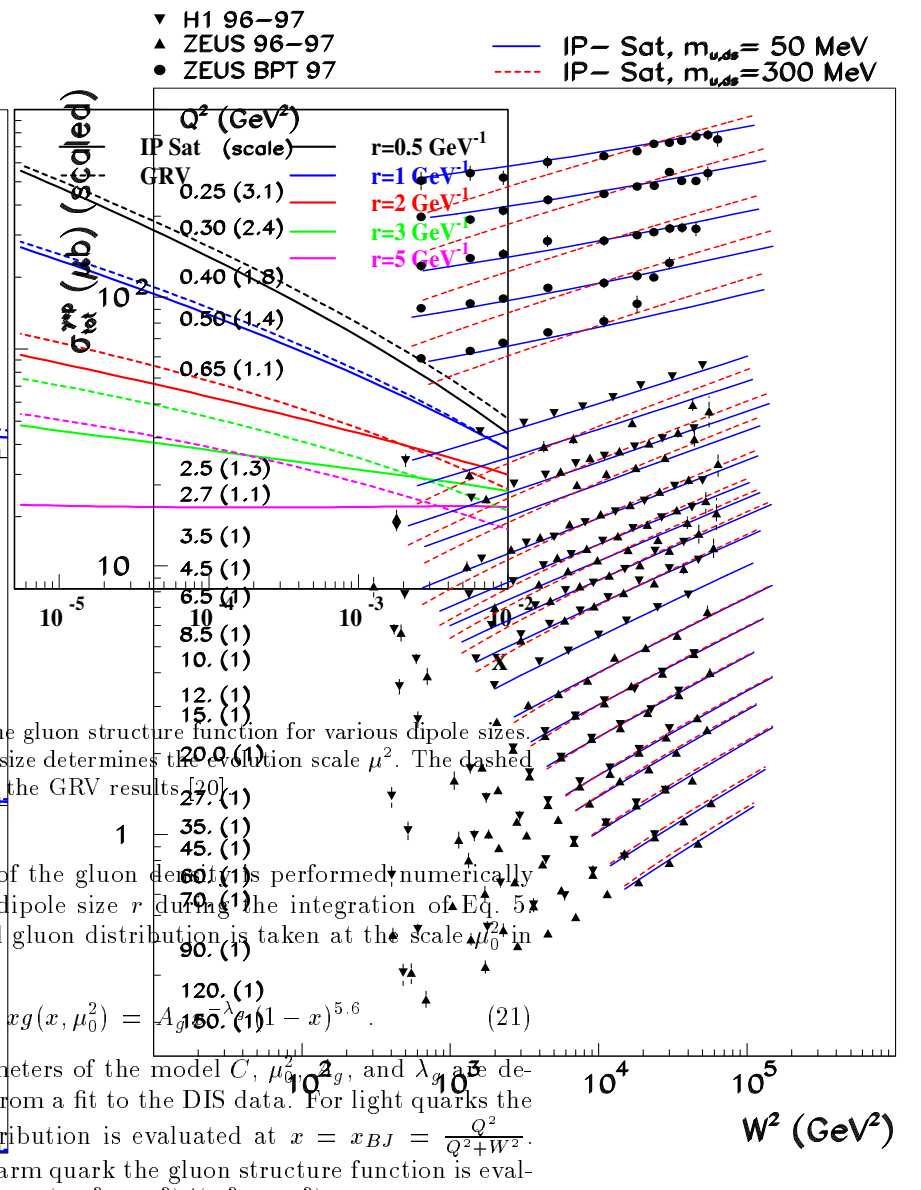


FIG. 9: The $\gamma^* p$ cross section as a function of $W^2$ at various $Q^2$. The values of $Q^2$ are shown on the left side of the plot along with the scale factor applied to the data for a better visibility. The full (dashed) line shows a fit by the IP Saturation Model with $m_{u,d,s} = 50$ MeV ($m_{u,d,s} = 300$ MeV). The fits are performed for $x < 0.01$.

scatters off the proton. Note that at smallest $Q^2$ and $r = 10^{-3}$ the majority of dipoles are smaller than $r \lesssim 2$ GeV$^{-1}$ and thus half of the dipoles are perturbative.

## IV. RESULTS FOR $\gamma^* p$ PROCESSES

### A. Inclusive total cross-section

The fit to the total $\gamma^* p$ cross-section data was performed in the range $x < 0.01$ and $Q^2 > 0.25$ GeV$^2$. The small $x$ cut leads to an upper limit on $Q^2$, $Q^2 < 200$ GeV$^2$. Figure 9 shows the $\gamma^* p$ cross section as a function of $W^2$ at the various $Q^2$ measured by the HERA experiments [29]. Following the rise of the total cross section with $W^2$ at fixed $Q^2$, we observe a striking change: for small $Q^2$ (the top of Fig. 9) the cross section rises slowly with the center of mass energy $W^2$, while for large $Q^2$ (the bottom of Fig. 9) the cross section rises strongly. If

### G. Dipole size

To interpret the IP Saturation model physically, we determined the typical dipole size contributing to the total cross-section. The distribution of dipole sizes $\frac{1}{\sigma^{\gamma^* p}}\frac{d\sigma^{\gamma^* p}}{dr}$ is the integrand of Eq. 5 after the $z$ integration is performed. Figure 8 shows this distribution at representative values of $x$ and $Q^2$. For each illustrated $x$ and $Q^2$ the arrow indicates the median radius of a dipole which

**Model able to reproduce inclusive, diffractive, and exclusive differential cross sections with relatively few parameters. Some examples:**

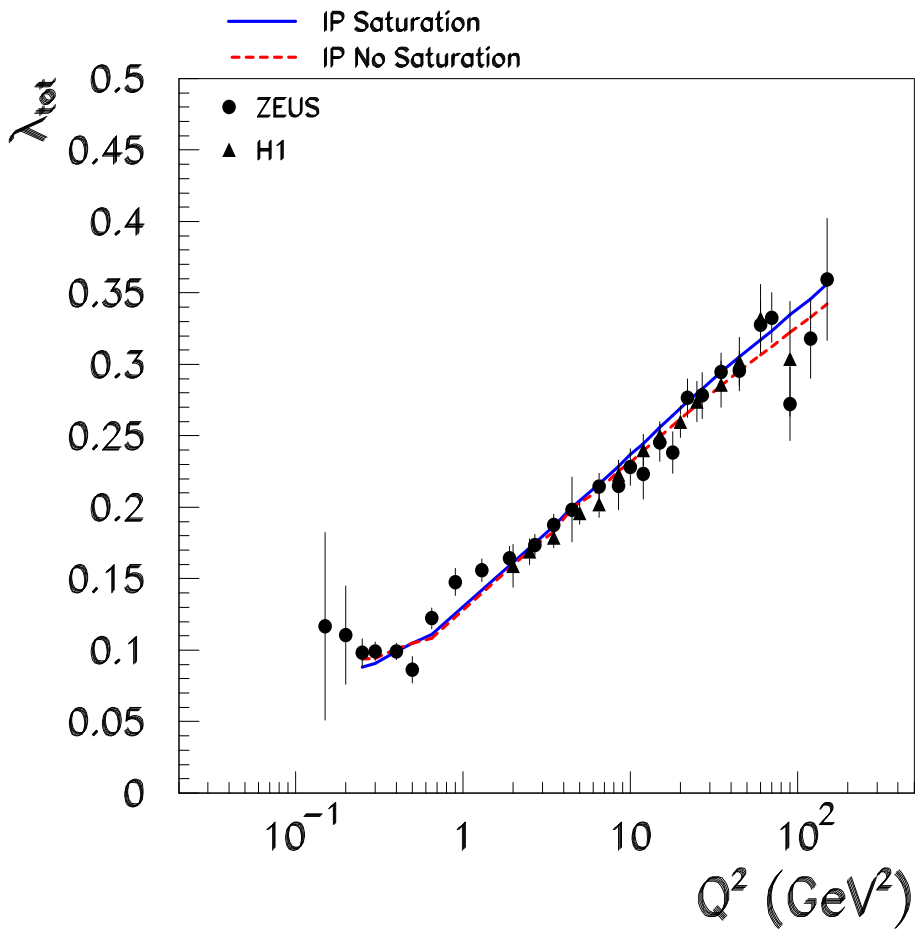


FIG. 10: The exponent $\lambda_{tot}$ as a function of $Q^2$. $\lambda_{tot}$ parametrizes the total cross section at fixed $Q^2$, $\sigma_{tot}^{\gamma^* p} \sim (1/x)^{\lambda_{tot}}$.

**The model is in many respects quite simple but quite successful at reproducing the data. Can we understand relationship of this approach to N$^k$LO DGLAP, BFKL, CCFM, … ?**

we parameterize the cross section by a power law

$$\sigma_{tot}^{\gamma^* p} \sim (W^2)^{\lambda_{tot}(Q^2)} \sim (1/x)^{\lambda_{tot}(Q^2)} , \qquad (31)$$

this change in the rate of rise from low to high $Q^2$ translates into a $Q^2$ dependence of the exponent $\lambda_{tot}$. $\lambda_{tot}(Q^2)$ is illustrated in Fig. 10 and summarizes one of the principle observations at HERA. At small $Q^2$, $\sigma_{\gamma^* p}$ increases with $W^2$ as in all hadronic reactions, $\lambda_{tot} \approx 0.08$ [30]. At at large $Q^2$ the exponent $\lambda_{tot}$ increases substantially.

In the IP Saturation model the increase of the exponent $\lambda_{tot}$ with $Q^2$ is a consequence of the DGLAP evolution. When the dipole size becomes smaller than $\sim \frac{2}{\mu_o}$ DGLAP evolution becomes increasingly effective and the growth of the gluon distribution at small $x$ becomes increasingly rapid. Mathematically speaking, $\lambda_{eff}$ increases for small size dipoles as seen in Fig. 5. Averaging over dipole sizes with the photon wave function translates $\lambda_{eff}(r)$ into $\lambda_{tot}(Q^2)$. The large increase in $\lambda_{tot}$ with $Q^2$ indicates a transition from a predominance of large to a predominance of small dipoles when evaluating the cross-section. The contribution of large dipoles at low $Q^2$ is determined by the light quark mass, $m_{u,d,s}$.

The parameters $A_g$, $\lambda_g$ and $\mu_0^2$ were found by fitting the total $\gamma^* p$ cross-section for various light quark masses. The parameter $C$ is strongly correlated to the parameters $A_g$ and $\lambda_g$ and does not affect the fit quality. Therefore, we set $C = 4$ by fiat. The mass of the charm quark was $m_c = 1.3$ GeV as required by elastic diffractive $J/\psi$ production discussed below. The results of the fits to the ZEUS data are collected in Table I. Because of the good agreement between the H1 and ZEUS data sets the com-

| $m_{u,d,s}$ (MeV) | $A_g$ | $\lambda_g$ | $\mu_0^2$ | $\chi^2$ |
|---|---|---|---|---|
| 300 | 1.67 | 0.226 | 6.85 | 70 |
| 150 | 2.34 | 0.043 | 1.32 | 19 |
| 100 | 2.85 | -0.04 | 0.96 | 15 |
| 50 | 3.47 | -0.12 | 0.77 | 13 |

TABLE I: Table of parameters determined in the total $\gamma^* p$ cross-section for different assumptions o quark mass $m_{u,d,s}$.

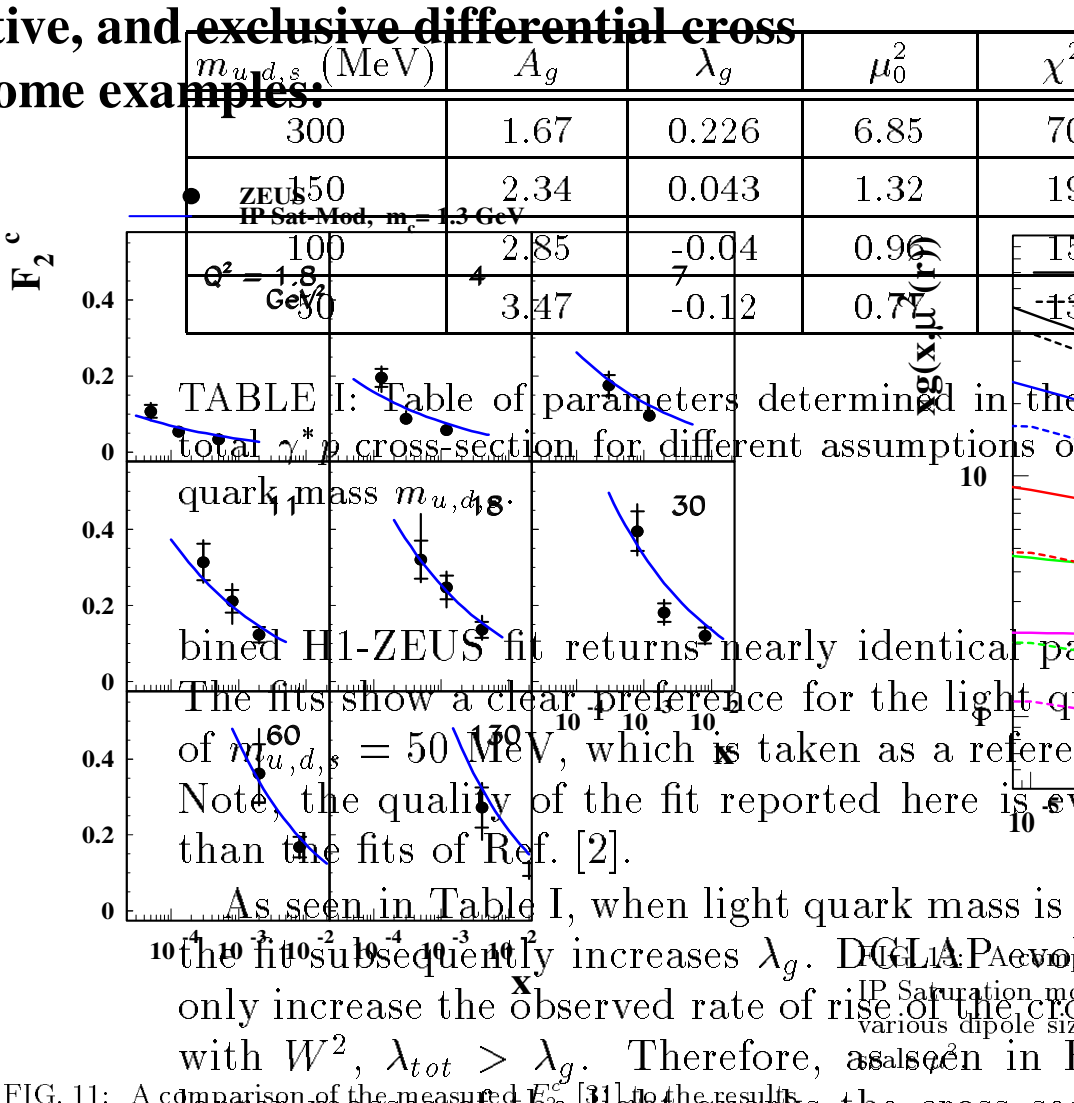


FIG. 11: A comparison of the measured $F_2^c$ [31] to the results of the model.

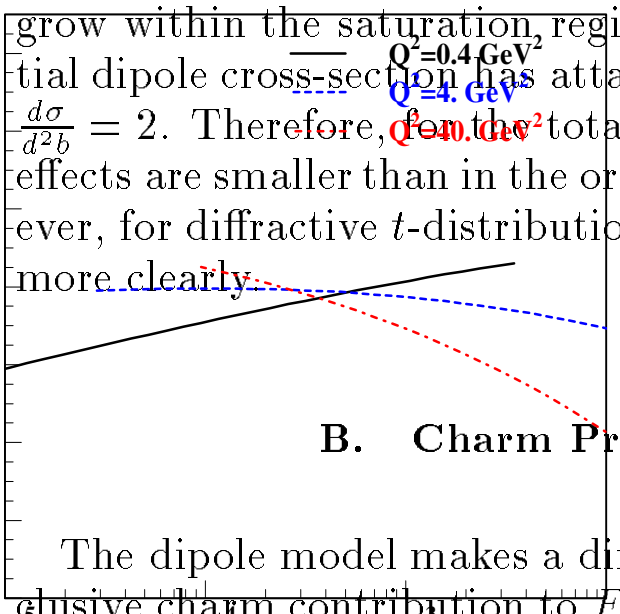


FIG. 12: The ratio $F_L/F_2$ as a function of $x$ at various photon virtualities.

bined H1-ZEUS fit returns nearly identical pa
The fits show a clear preference for the light q
of $m_{u,d,s} = 50$ MeV, which is taken as a refere
Note, the quality of the fit reported here is e
than the fits of Ref. [2].

As seen in Table I, when light quark mass is
the fit subsequently increases $\lambda_g$. DGLAP evo
only increase the observed rate of rise of the cr
with $W^2$, $\lambda_{tot} > \lambda_g$. Therefore, as seen in
larger masses of the light quarks the cross sec
too quickly with $W^2$ at low $Q^2$.

In contrast to the GBW model [8] and the
Ref. [2], saturation is not responsible for the
$\lambda_{tot}$ rise with $Q^2$ since the impact parameter is
This is because the total dipole cross section co
grow within the saturation region although th
tial dipole cross-section has attained its asymp
$\frac{d\sigma}{d^2b} = 2$. Therefore, for the total cross-section
effects are smaller than in the original GBW mo
ever, for diffractive $t$-distributions saturation
more clearly.

## B. Charm Production

The dipole model makes a direct prediction
clusive charm contribution to $F_2$. In the dipole
the charm quark distribution is calculated from
distribution. Figure 11 shows a comparison be
measured and predicted values of the charm
function $F_2^c$. The results depend weakly on
mass. The good agreement with data for bo
and H1 experiments [31, 32] confirms the cons
the model and supports the dipole picture.

## C. Determination of $F_L$

As a byproduct of our investigation we deter
longitudinal structure function $F_L$. A measu
$F_L$ would be a critical test of our understand
gluon distribution. $F_L$ is zero in the naive par
and is non-zero only after gluon radiation is in
dipole models at small $x$, both $F_L$ and $F_2$ are
by the gluon distribution and therefore they be
larly. Figure 12 shows the ratio of $F_L$ to $F_2$ as

# More detailed tests of radiation in QCD: forward jets

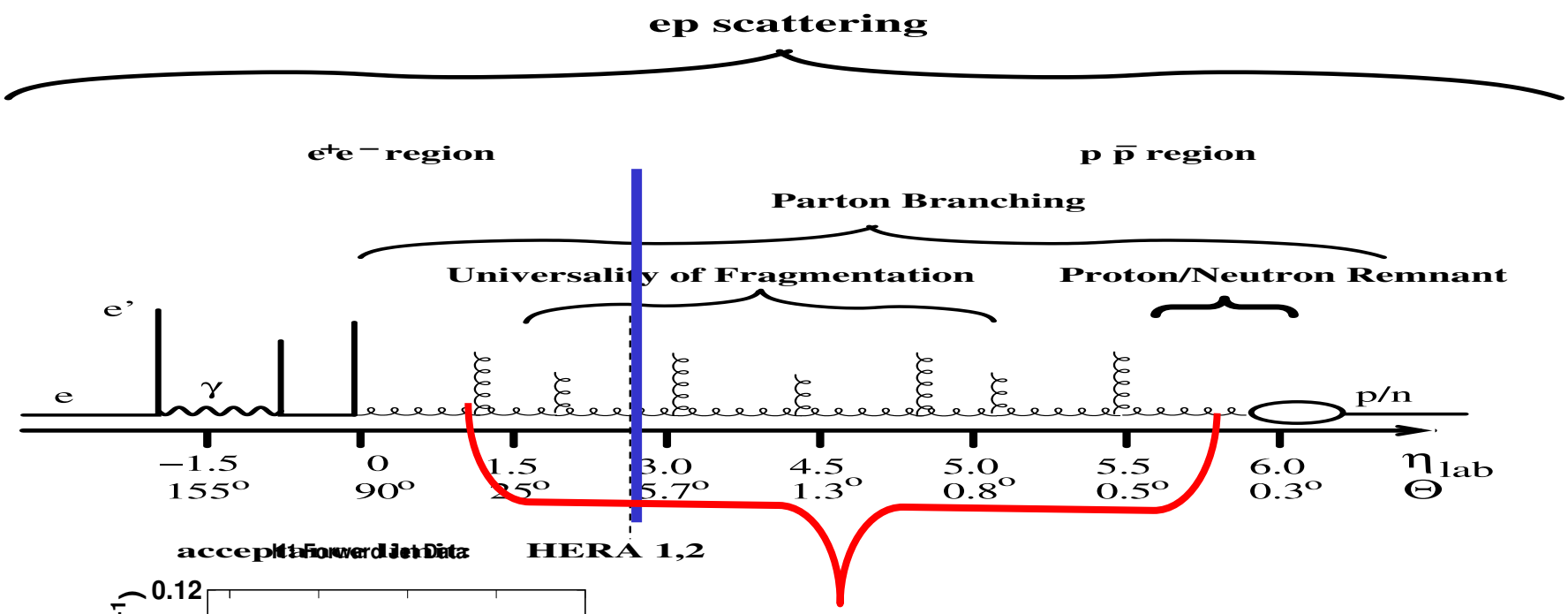


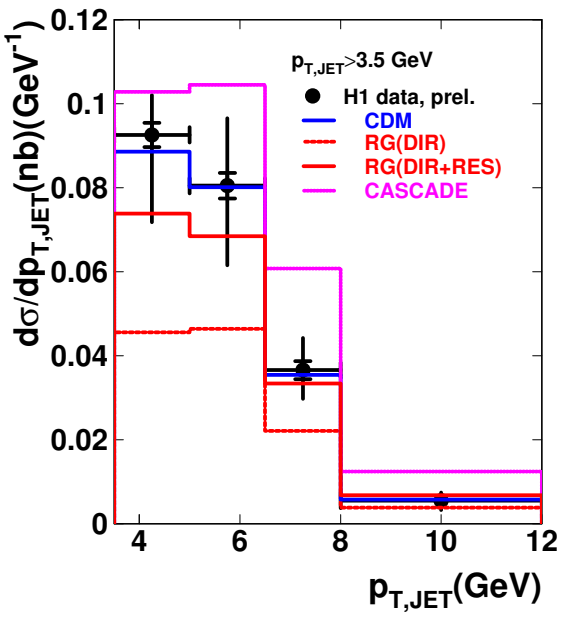


## Investigate this region

**Large effects are expected in Forward jet cross sections at high rapidities (also for forward particle production (strange, charm, …)**

# Open Questions – Next Steps

**• Measure the behavior of inclusive, diffractive and exclusive reactions in the region near $Q^2$=1 $GeV^2$ to understand parton to hadron transition.**

**• Measure $F_L$ over widest possible kinematic range, as this is a crucial observable for testing our understanding of radiation processes in QCD.**

**• Measure exclusive processes (VM production, DVCS) over wide W range to precisely pin down energy dependence of cross section. Need t-dependence of cross sections to get 3-D map of proton.**

**• Measure forward jet cross sections over widest possible rapidity range, to study radiation processes over the full rapidity range from the proton to the scattered quark.**

**• AND, do it all with nuclei !**

# Precision eA measurements

- **Enhancement of possible nonlinear effects (saturation)**

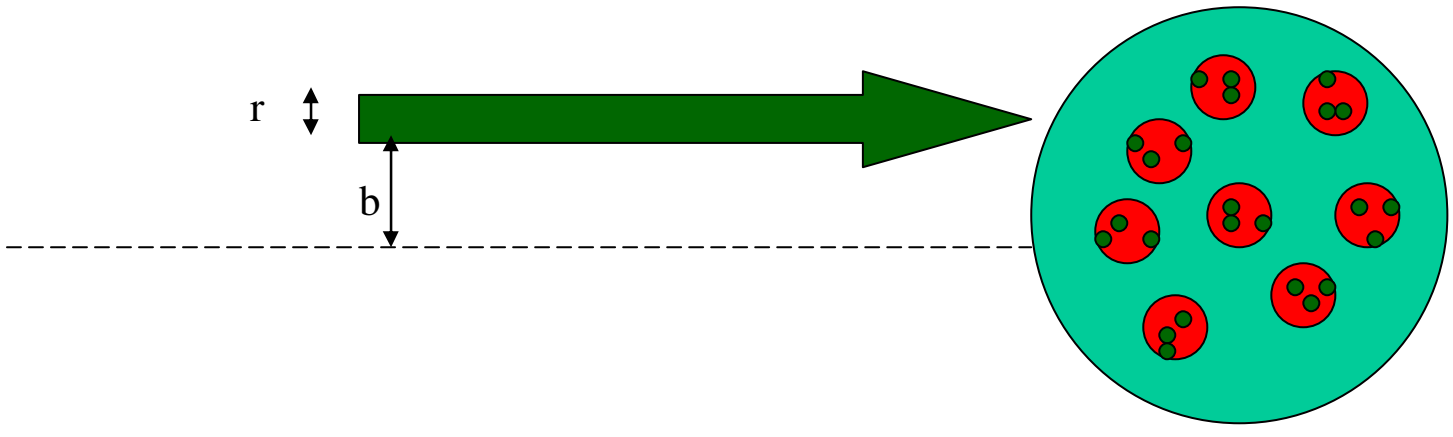


**At small x, the scattering is coherent over nucleus, so the diquark sees much larger # of partons:**

$xg(x_{eff},Q^2) = A^{1/3}\, xg(x,Q^2)$, **at small-x,** $xg \propto x^{-\lambda}$, **so**

$x_{eff}^{-\lambda} = A^{1/3} x^{-\lambda}$ **so** $x_{eff} \approx xA^{-1/3\,\lambda} = xA^{-3}\ (Q^2 < 1\ \mathrm{GeV}^2)$

$= xA^{-1}\ (Q^2 \approx 100\ \mathrm{GeV}^2)$

# Parton densities in nuclei

**Early RHIC data is well described by the Color Glass Condensate model, which assumes a condensation of the gluon density at a saturation scale $Q_S$ which is near (in ?) the perturbatively calculable regime. Properties of such a color glass can be calculated from first principles (Mc Lerran-Venugopalan). Closely connected to dipole model approach.**

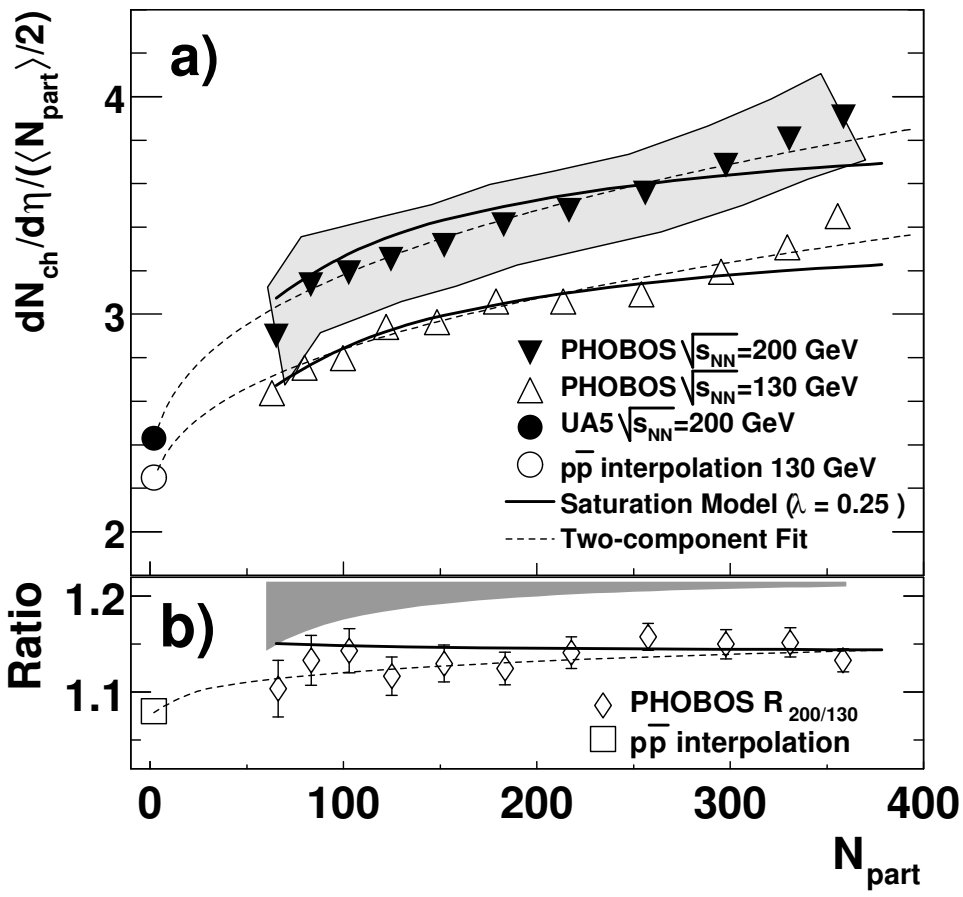


**The same basic measurements ($F_2$, $F_L$, $dF_2/d \ln Q^2$, exclusive processes) are needed for understanding parton densities in nuclei.**

# What about HERA-2

- **The goal of HERA -2 is to deliver 1 fb $^{-1}$/expt, divided into e $^{-}$,e $^{+}$ and L,R handed lepton polarization.**
- **The physics goal i s the extraction of high -x,Q $^{2}$ parton densities, measurement of EW parameters, high P $_{T}$ processes, and searches for new physics.**
- **The H1 and ZEUS detectors were designed for this**

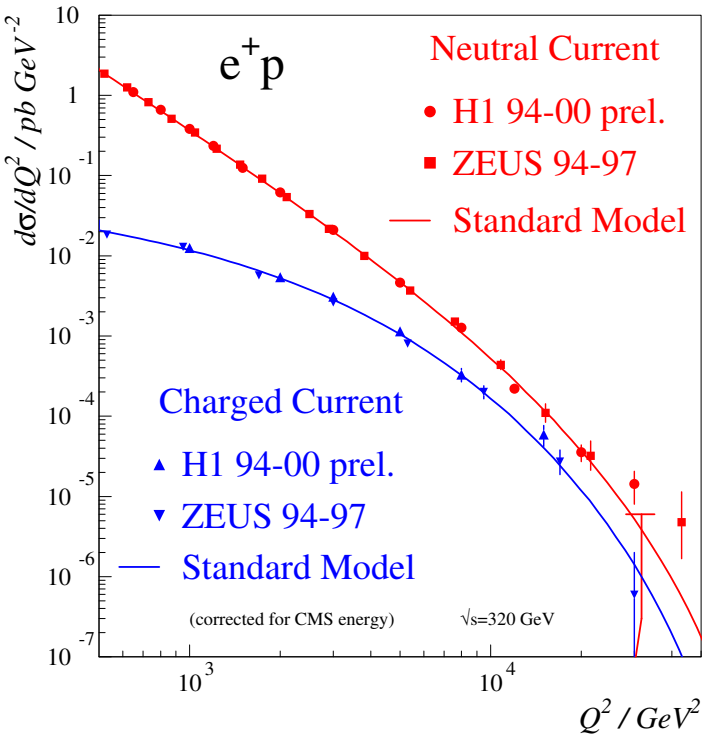


**EW unification in one plot – measured with HERA -1. Few K CC events. The upgraded luminosity, and different polarizations, will yield precise tests of EW and flavor dependent valence quark densities.**

# A new detector to study strong interaction physics

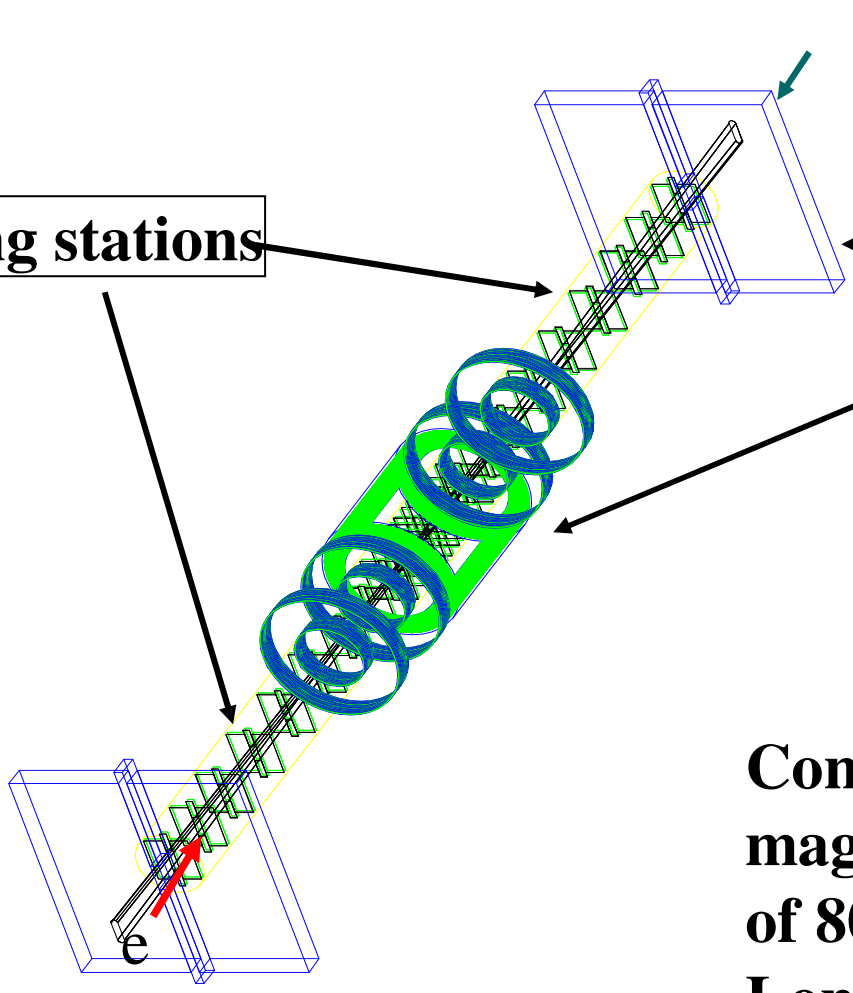


**Compact – fits in dipole magnet with inner radius of 80 cm.**
**Long - $|z| \leq 5$ m**

**The focus of the detector is on providing complete acceptance in the low $Q^2$ region where we want to probe the transition between partons and more complicated objects.**

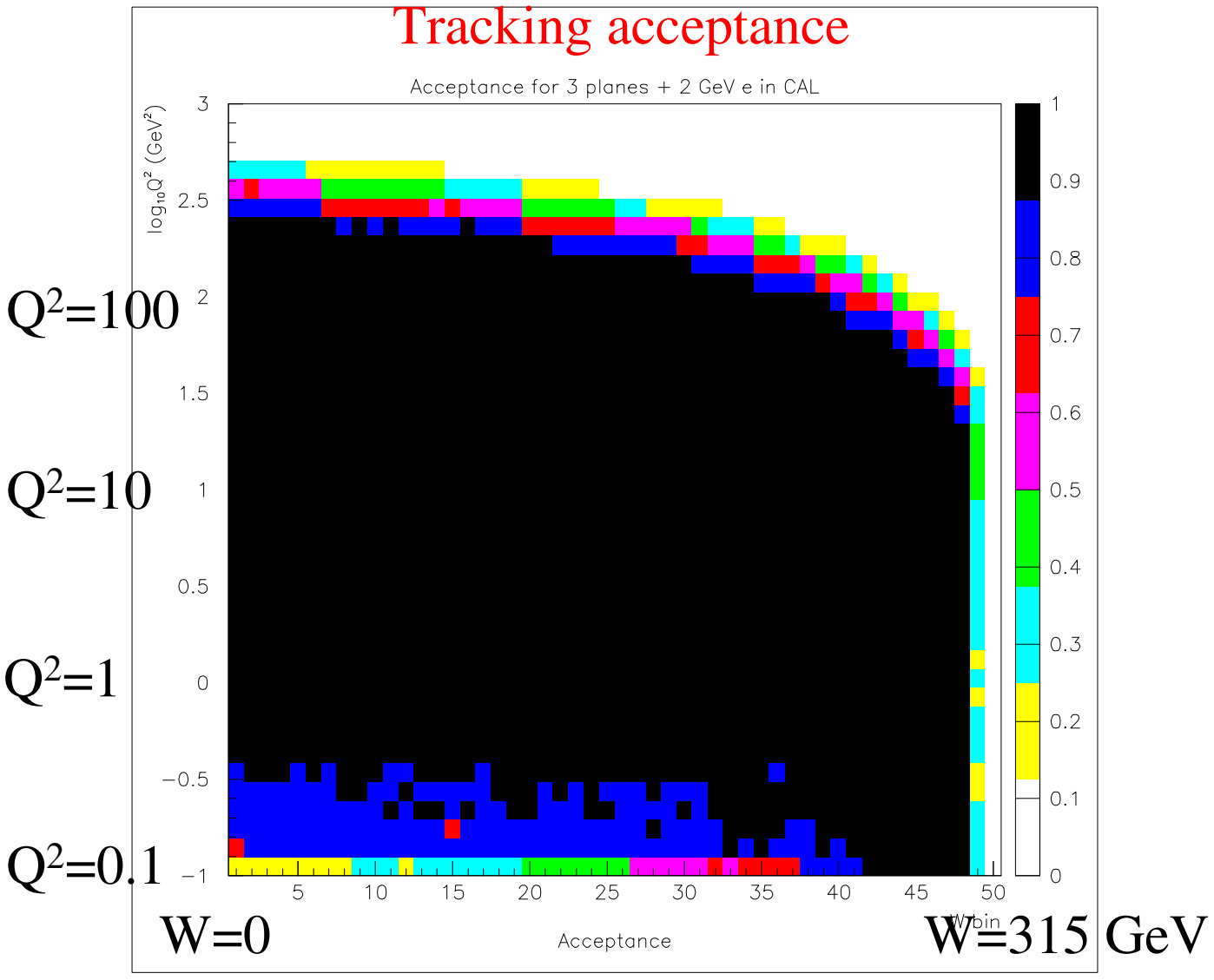

## Tracking acceptance in proton direction

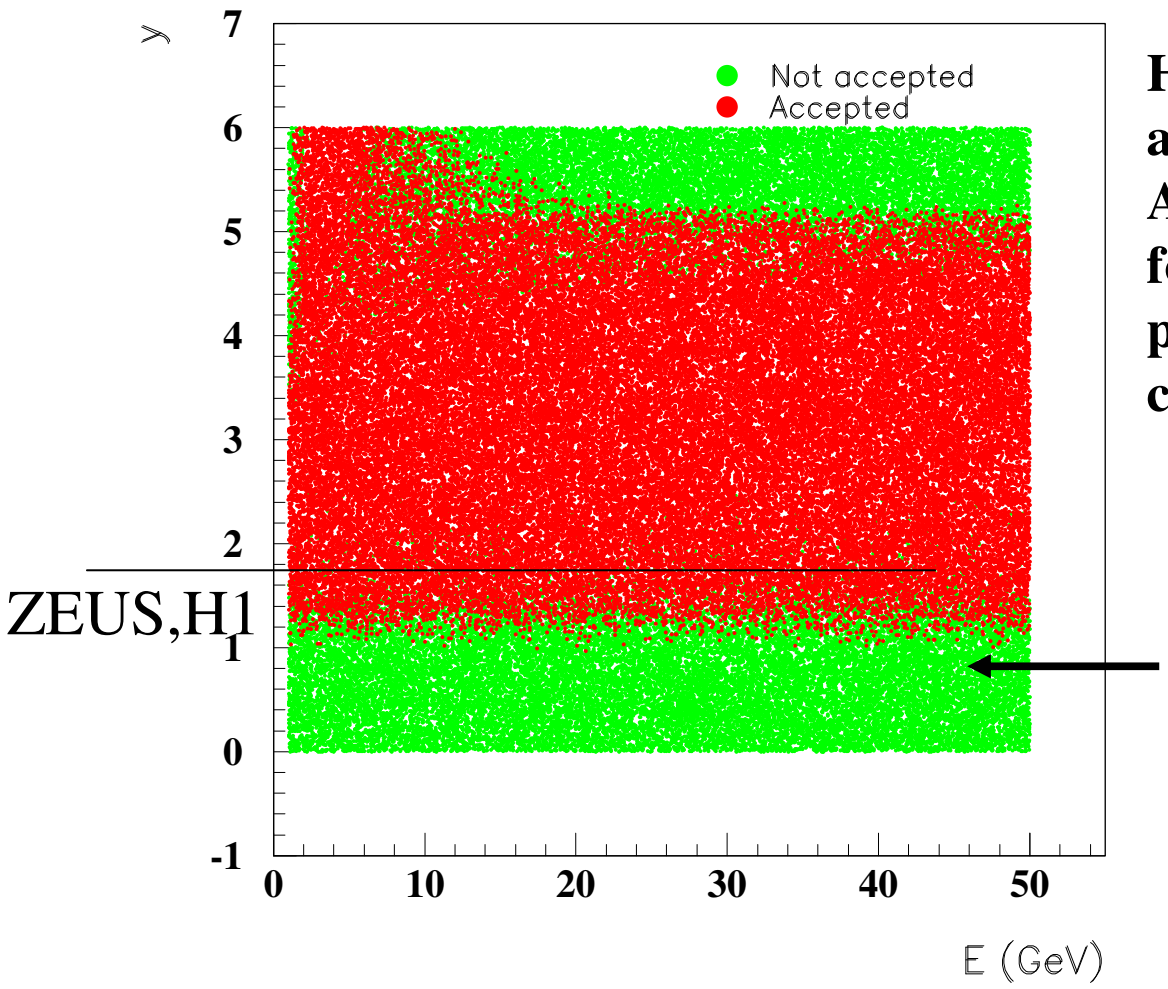


**Huge increase in tracking acceptance compared to H1 And ZEUS. Very important for forward jet, particle production, particle correlation studies.**

**This region covered by calorimetry**

**Accepted ≡ 4 Si stations crossed.**

**Tracking detector: very wide rapidity acceptance, few % momentum resolution in 'standard design' over most of rapidity range.**

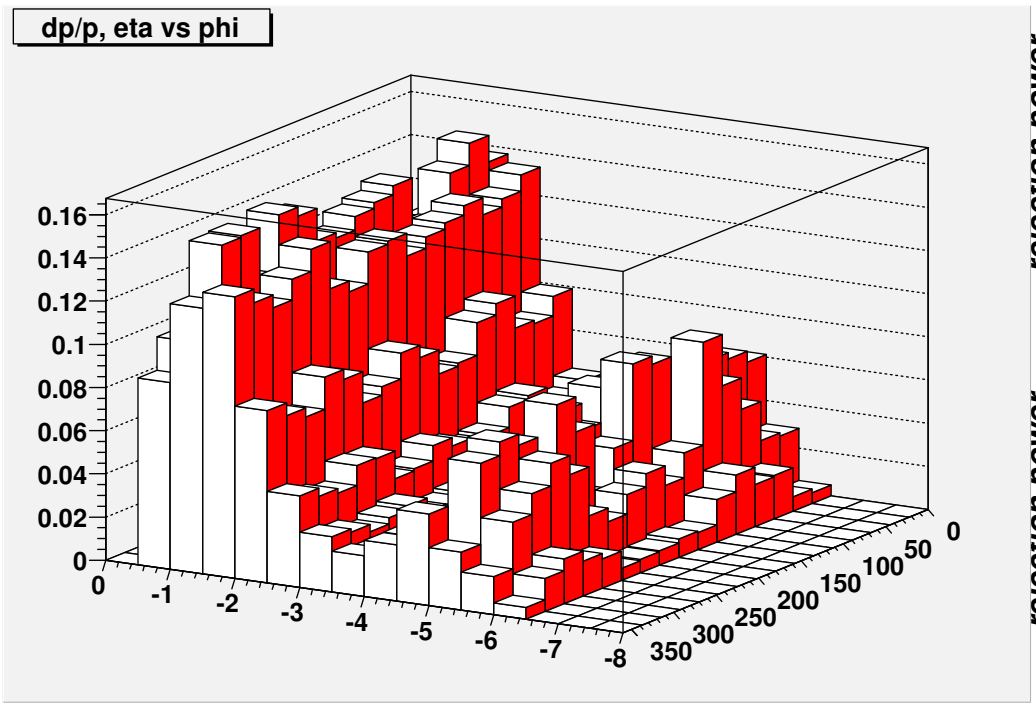


## e/π separation study

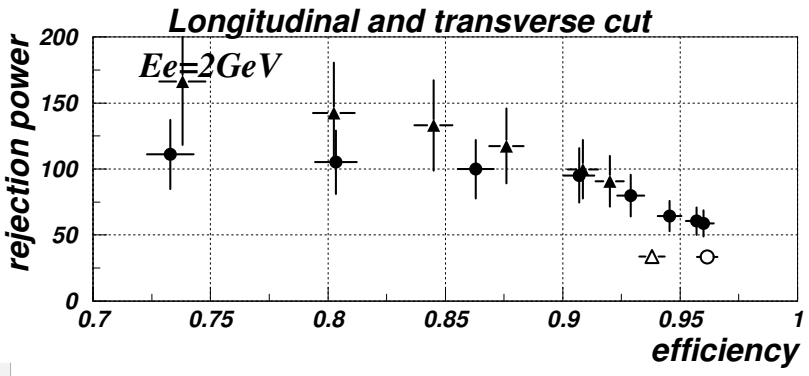


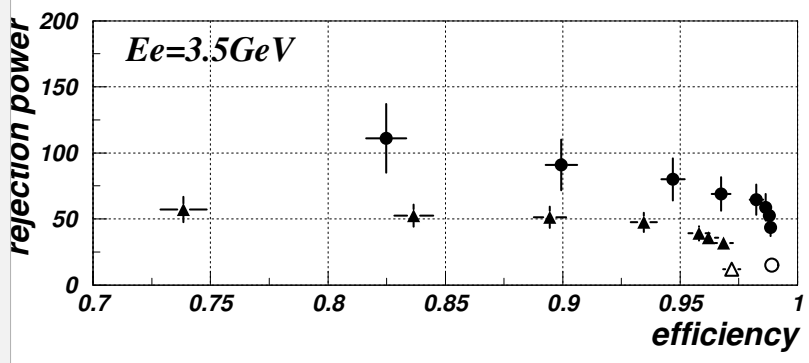


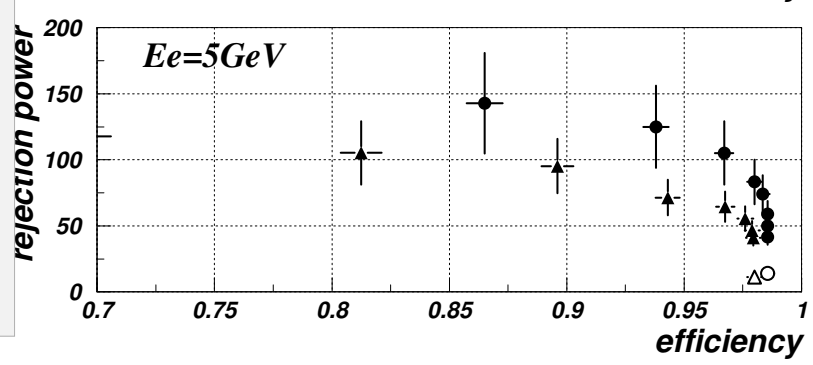


**Aim for 2 GeV electron ID**

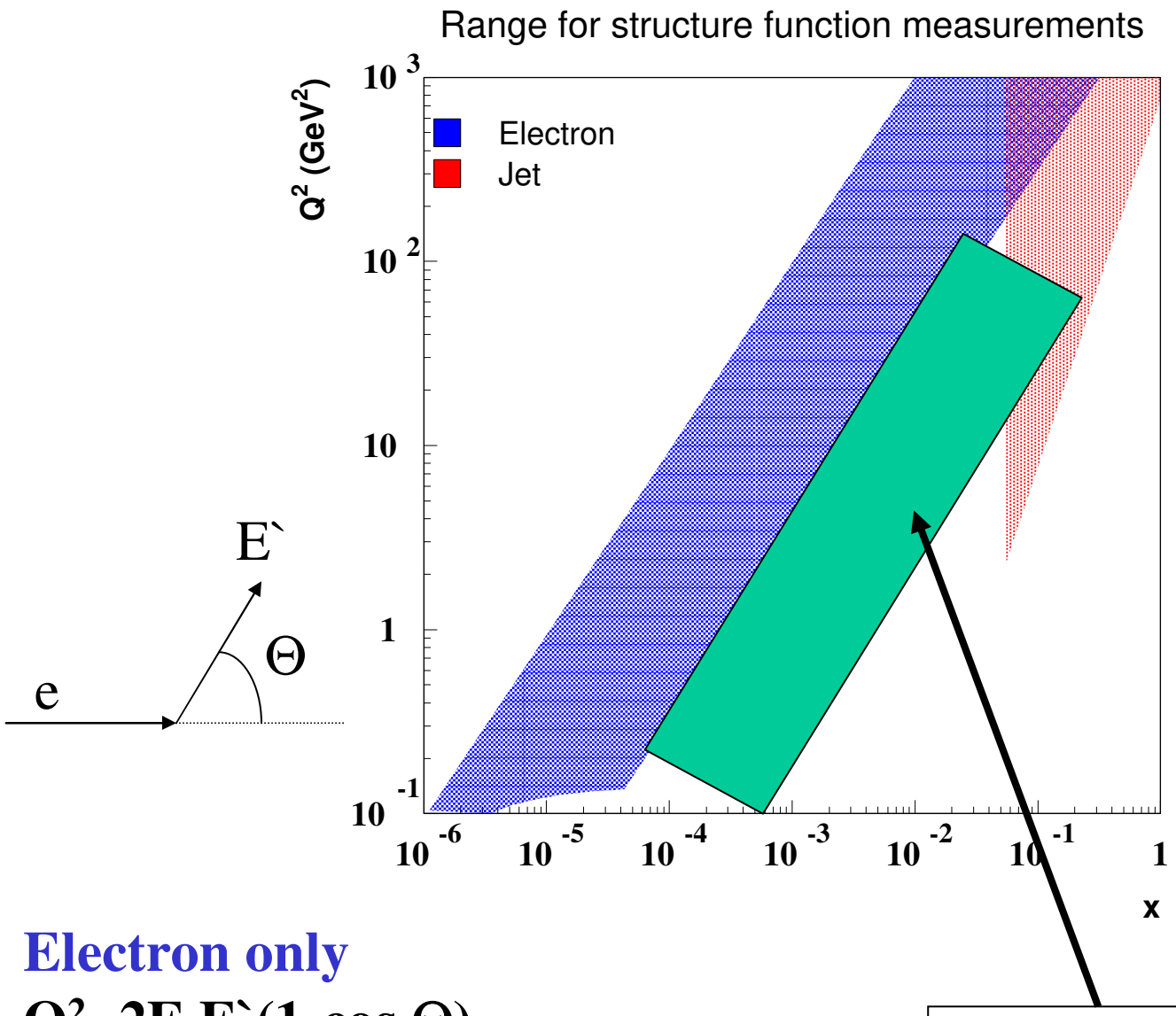


**Nominal beam energies**

**Jet method:**
**Jet energy yields x via**
**$x = E_{jet}/E_P$**

**Electron only**

**$Q^2=2E\,E`(1-\cos\Theta)$**
**$y = 1-E`/2E(1+\cos\Theta)$**
**$x = Q^2/sy$  $dx/x \approx 1/y\ dp/p$**

**Mixed method in between – needs studies**

$$d^2\sigma/dxdQ^2=2\pi\alpha^2/xQ^4[\ (1+(1-y)^2)F_2(x,Q^2) - y^2F_L(x,Q^2)\ ]$$

**Fix x, $Q^2$. Use different beam energies to vary y. Critical issue: e/π separation**

**$F_L$ can be measured precisely in the region of maximum interest. This will be a strong test of our understanding of QCD radiation.**

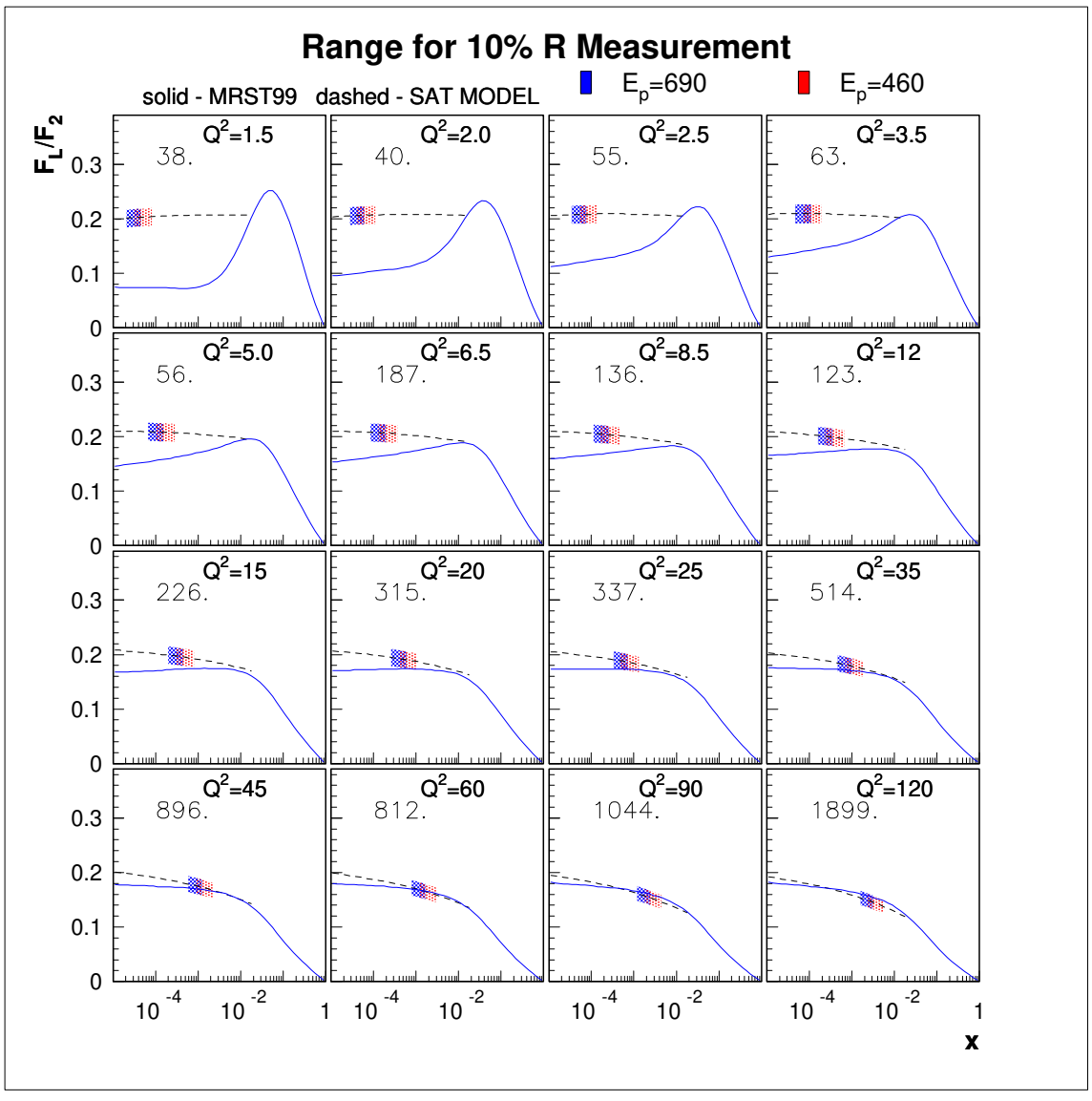

Range for structure function measurements

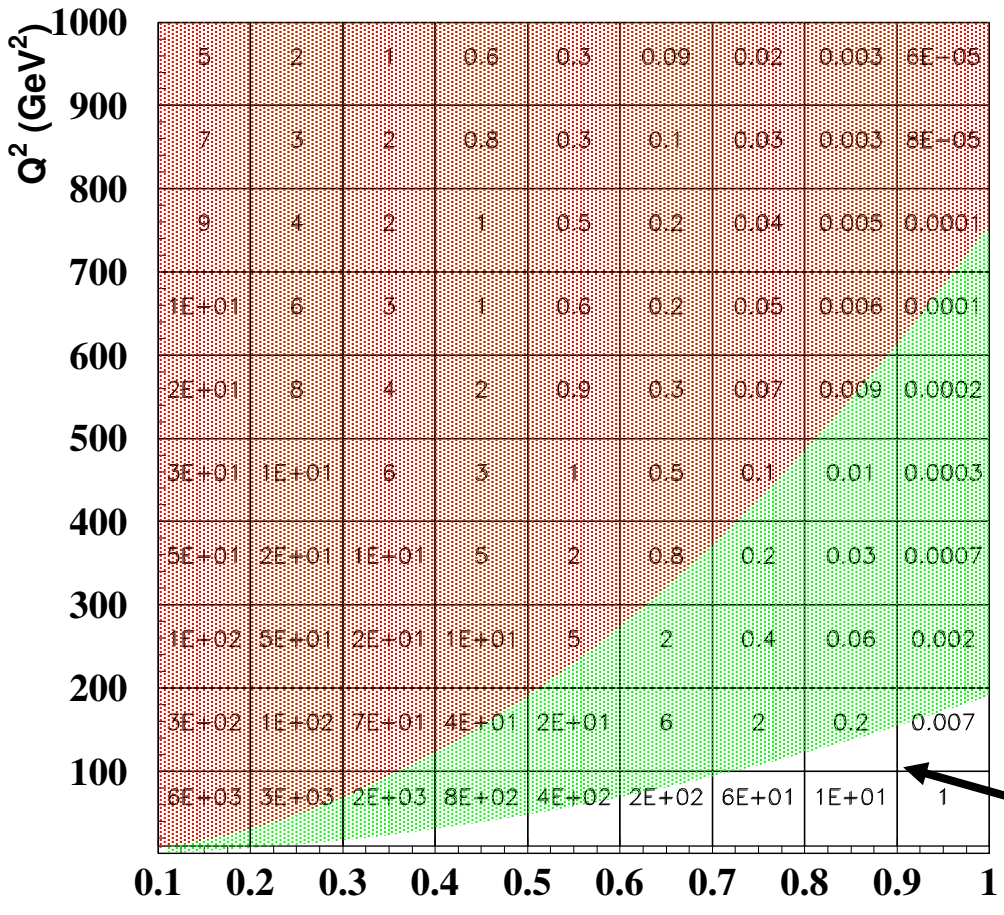


**Cross sections calculated from ALLM**

**Very forward calorimeter allows measurement of high energy, forward jets, and access to high-x events at moderate $Q^2$**

**Integral of $F_2(x,Q^2)$ up to x=1 known from electron information**

**Forward jet cross sections: see almost full cross section !**

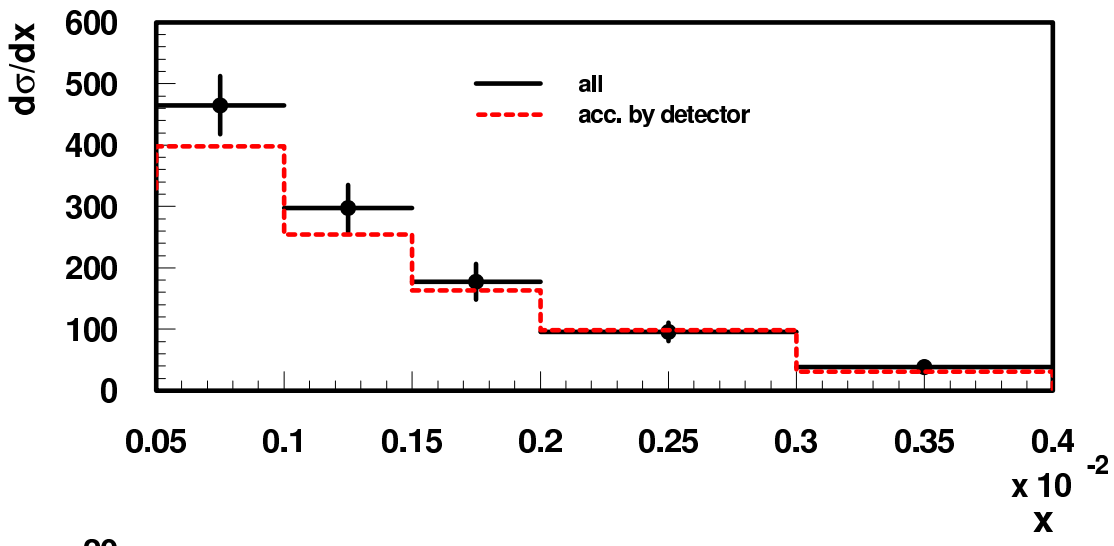


**Range covered by H1, ZEUS**

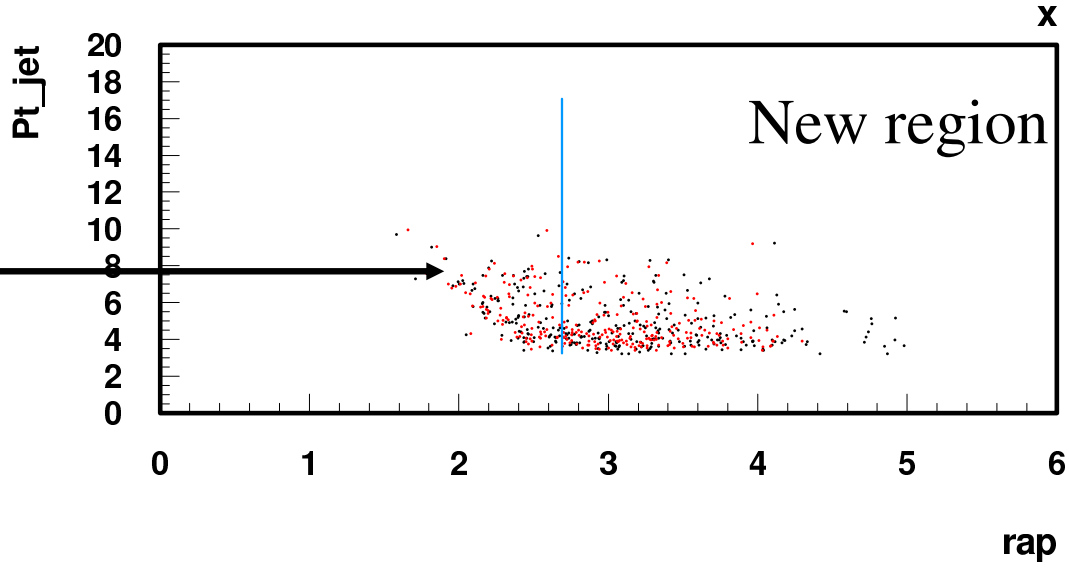

**Very large gain also for vector meson, DVCS studies. Can measure cross sections at small, large W, get much more precise determination of the energy dependence.**

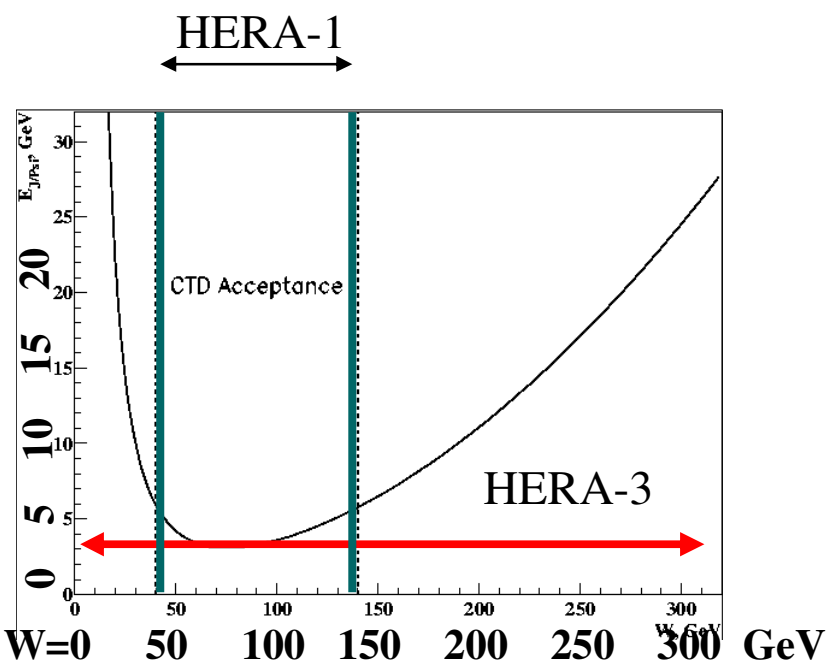


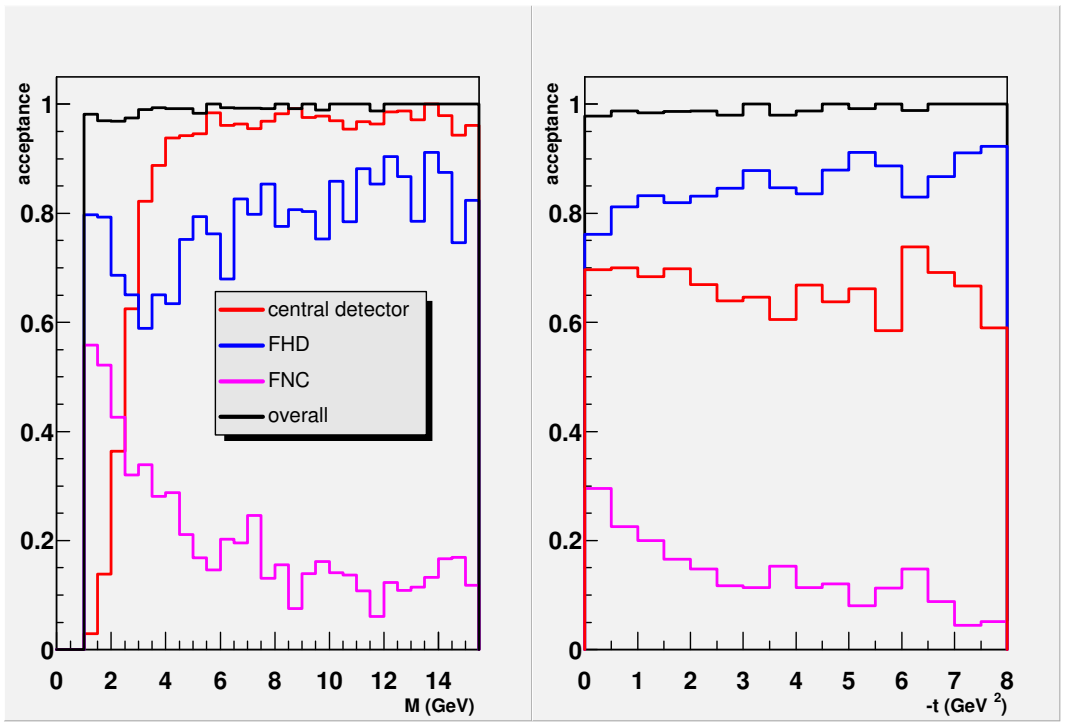


**Can also get rid of proton dissociation background by good choice of tagger:**

**FHD- hadron CAL around proton pipe at z=20m**

**FNC-neutron CAL at z=100m**

# Summary

• **Existing data ($F_2$ fits, forward jets,+…) show limitations of pQCD calculations. Transition region observed.**
• **Exciting theoretical developments over the past few years. We are approaching a much deeper understanding of the high energy limit of QCD.**

**⇒ Measure with more precision, over wider kinematical range, to see where/how breakdown takes place (high rapidities, high-t exclusive processes, expanded W, $M_X$ range for diffraction, full coverage of transistion region)**

**⇒ Precision $F_L$ measurement: key observable for pinning down pQCD. Large differences in predictions at LO, NLO, NNLO, dipole model.**

**⇒ eD, eA measurements to probe high density gluon state, parton densities for nuclei.**

• **Additional benefits: parton densities for particle, astroparticle and nuclear high energy physics experiments. Crucial for cross section calculations.**

# Summary-continued

**The ZEUS and H1 detectors were not designed with this physics in mind. An optimized detector would greatly enhance the sensitivity of the measurements to deviations from pQCD !**

**Experiment would focus on full acceptance in the small angle electron and proton directions. Centered on precision tracking and EM calorimetry.**

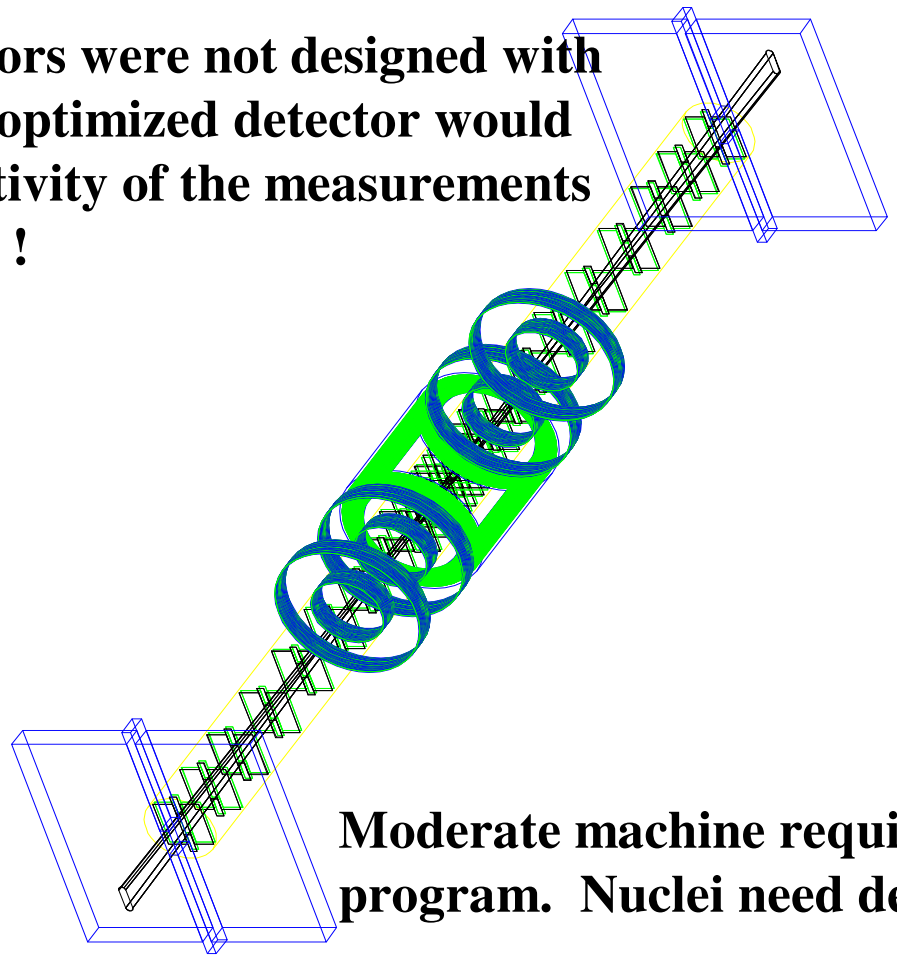

**Moderate machine requirements for eP program. Nuclei need developments.**

**Let's take advantage of the full potential of HERA to answer some fundamental questions about our universe !**